

## Abstract

Psf2, a member of the heterotetrameric GINS Complex, plays a role in cell cycle progression and maintenance of genomic integrity

By Laura M Henderson

July 8, 2010

Director: Tim Christensen

Multiple proteins are involved in the complete and accurate replication of the genome during S phase of the cell cycle. At the G1/S phase transition, the heterotetrameric GINS complex is recruited to the origin, and facilitates the helicase activity of the Mcm2-7 complex. Each of the four subunits of the GINS complex is essential for proper completion of DNA replication initiation and elongation. Inaccurate replication of the genome results in a multitude of disease states, specifically, cancer.

Psf2, a subunit of the GINS complex, has been previously implicated in the segregation of chromosomes during M phase. Additionally, it has been shown that reduced levels of Psf2 in yeast results in stalled replication forks and incomplete DNA replication. However, to date, the function of Psf2 in higher eukaryotes has only been studied in tissue culture models. To provide insight into the role of Psf2 in a multicellular organism, we used an *in vivo* approach to characterize the phenotypes resulting from the C-terminal truncation of Psf2 in a homozygous lethal mutant in *Drosophila*. Through analysis of larval brain tissue, salivary tissue, ovarioles, and embryonic tissue, we found the mutant Psf2 displays defects during M phase of the cell cycle and DNA replication in endoreplicating cells. Curiously, the RNAi knockdown of Psf2 results in a defect in S phase of the cell cycle, with no effects on M phase. Therefore, we hypothesize that Psf2 plays an essential role in cell cycle progression. Additionally, removal of the C-terminal domain is essential for either the correct formation of the GINS complex, or for an external interaction, possibly with checkpoint or chromosome segregation proteins.



*Psf2*, a subunit of the heterotetrameric GINS complex, plays a role in cell cycle progression and maintenance of genomic integrity

A Thesis

Presented to

The Faculty of the Department of Biology  
East Carolina University

In Partial Fulfillment

Of the Requirements for the Degree  
Master's of Science in Biology

By Laura M Henderson

July 8, 2010

©Copyright 2010  
Laura M Henderson

*Psf2*, a member of the heterotetrameric GINS Complex, plays a role in cell cycle progression and maintenance of genomic integrity

By Laura M Henderson

Approved by:

Thesis Director: \_\_\_\_\_

Tim W. Christensen, Ph.D

Committee Member: \_\_\_\_\_

Anthony Capehart, Ph.D

Committee Member: \_\_\_\_\_

Carol Goodwillie, Ph.D

Committee Member: \_\_\_\_\_

Brian Shewchuk, Ph.D

Chair, Department of Biology: \_\_\_\_\_

Jeff McKinnon, Ph.D

Dean of Graduate School: \_\_\_\_\_

Paul J. Gemperline, Ph.D

## Acknowledgements

I would like to offer thanks to Tim Christensen for his ideas, help and support throughout this project and the completion of my Master's degree. Secondly, I would like to thank the members of my committee: Anthony Capehart, Carol Goodwillie, and Brian Shewchuk for their excellent advice throughout this process. Jen Apper, Michael Reubens, Brian Sufrinko, Catherine Gouge, Chad Hunter, Lena Keller, William Whited, Wayne Rummings and Tabitha Reel for their help in lab. Additionally, I would like to thank Tom Fink for all his help and hard work in the imaging core. Finally I would like to thank East Carolina University and the Department of Biology as well as my family and friends for all of their support.

## Table of Contents

List of Tables.....	x
List of Figures.....	xi
Chapter 1: Introduction.....	1
I. Background .....	1
a.DNA Replication.....	1
b.GINS Complex.....	2
II. Specific Aims .....	3
III. Materials and Methods .....	4
Chapter 2: Results.....	16
V. Discussion.....	27
VI. Conclusion .....	33
VII. References.....	36
VIII. Appendix I .....	41
IX. Appendix II .....	44
X. Appendix III .....	46
XI. Appendix IV .....	48
XII. Appendix V .....	49
XIII. Appendix VI .....	53

## **List of Tables**

<b>Components of Buffer A.....</b>	<b>17</b>
<b>Components of Buffer B .....</b>	<b>17</b>
<b>Components Added for PCR .....</b>	<b>18</b>
<b>Primers Used to Amplify Psf2 .....</b>	<b>18</b>
<b>Components Added for Entry Vector Cloning .....</b>	<b>20</b>
<b>Components Added for Destination Vector Cloning .....</b>	<b>20</b>
<b>Components of 10X HEPES Running Buffer.....</b>	<b>51</b>
<b>Components of Transfer Buffer .....</b>	<b>52</b>
<b>Components of Washing Buffer .....</b>	<b>52</b>

## List of Figures

Schematic Diagram of Eukaryotic Cell Cycle .....	10
Replication Initiation Complex Formation .....	11
Crystal Structure of the Human GINS Complex .....	13
Crystal Structure of Psf2 .....	13
Structure of the Psf2 Protein .....	15
Generation of the Transgenic Fly .....	21
Generation of Rescue Fly .....	22
Generation of Homozygous Mutant Fly .....	22
Homozygous Mutant Late Embryonic Arrest Visualization .....	28
Mitotic Index of <i>psf2</i> Heterozygous Mutant .....	28
Defects Chromosome Dynamics Visualized in Larval Brains .....	29
EdU Incorporation in <i>psf2</i> Heterozygous Larval Brains .....	30
Defects Visualized in Homozygous <i>psf2</i> Early Embryos .....	31
Heterozygous <i>psf2</i> Mutants Display Defects in Salivary Tissue .....	32
<i>psf2</i> Heterozygous Mutants Display Defects in Ovariole Development .....	34
RNAi Knockdown of Psf2 Leads to an S Phase Delay .....	36
Yeast Two-Hybrid Analysis of Psf2 Interactions .....	38
Schematic Model of Possible Psf2 Mutant Scenarios .....	42
Western Blot of Psf2 .....	51
Condensation Defects Visualized in Mcm10 Mutant Ovarioles .....	54
Mutated Eye Region Resulting from Psf2 RNAi Knockdown .....	55
Generation of a Psf2 null mutant using imprecise p-element excision .....	57
Generation of Psf2-Psf1 double mutant fly .....	58
Generation of Psf2-Sld5 double mutant fly .....	59
Generation of Psf2-Mcm2 double mutant fly .....	60
Generation of PEV Fly Line .....	62
Position Effect Variegation Analysis of Psf2 .....	63

# Chapter 1: Introduction

## I. Background

### a. DNA Replication

In order to maintain viability, each cell must insure accurate and complete replication of its genome within a crucial time frame (1). Deviation from this innate process leads to multiple complications for the cell ranging from mutations to death (2). Eukaryotic cells have developed controls to prevent mis-regulation of the cell cycle along with checkpoints to ensure maintenance of genomic integrity (3).

The growth, development and proliferation of a cell rely on the correct progression of the eukaryotic cell cycle. After dividing, a daughter cell enters G<sub>1</sub> phase (Figure 1), or the first growth phase of the cell cycle. This phase is characterized by expansion of the cytoplasm and an increase in organelles. During early G<sub>1</sub> phase, the ground work for DNA replication is laid down with the recruitment of over 20 replication proteins onto specific sites on the DNA. The process begins with the Origin Recognition Complex (ORC), a six subunit complex, which scans the double stranded DNA for AT rich sequences, where it binds and recruits other essential

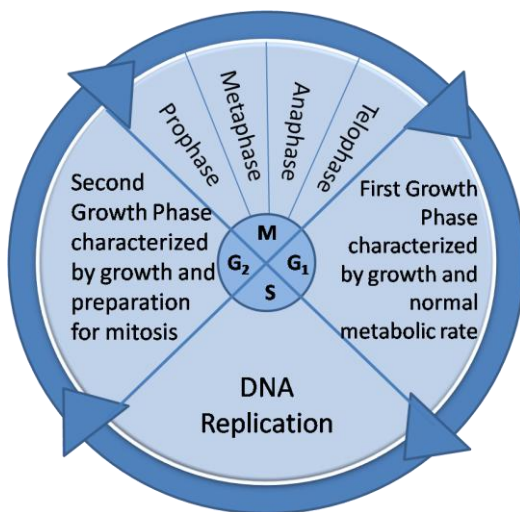


**Figure 1.** Schematic diagram of the eukaryotic cell cycle.

replication proteins (4). Also recruited with ORC is Cdc6,

which, in turn, is essential for the association of yet more replication proteins (Figure 2a) (5). After the recruitment of ORC and Cdc6 to the origin, another protein, Dup, is required for the loading of the helicase complex. At the start of G1, Geminin is bound to Dup, inhibiting the activation of helicase recruitment. Once Geminin is degraded, Dup is activated and recruited to the origin (6). Upon the binding of these three proteins, Mcm2-7 is loaded onto the origin (7). Mcm2-7 is a 6 subunit ring hypothesized to contain helicase activity (8). After Mcm2-7 is recruited to the origin, another mini-chromosome maintenance protein, Mcm10, also joins, creating the Pre-Replication Complex (Pre-RC) (Figure 2b) (9).

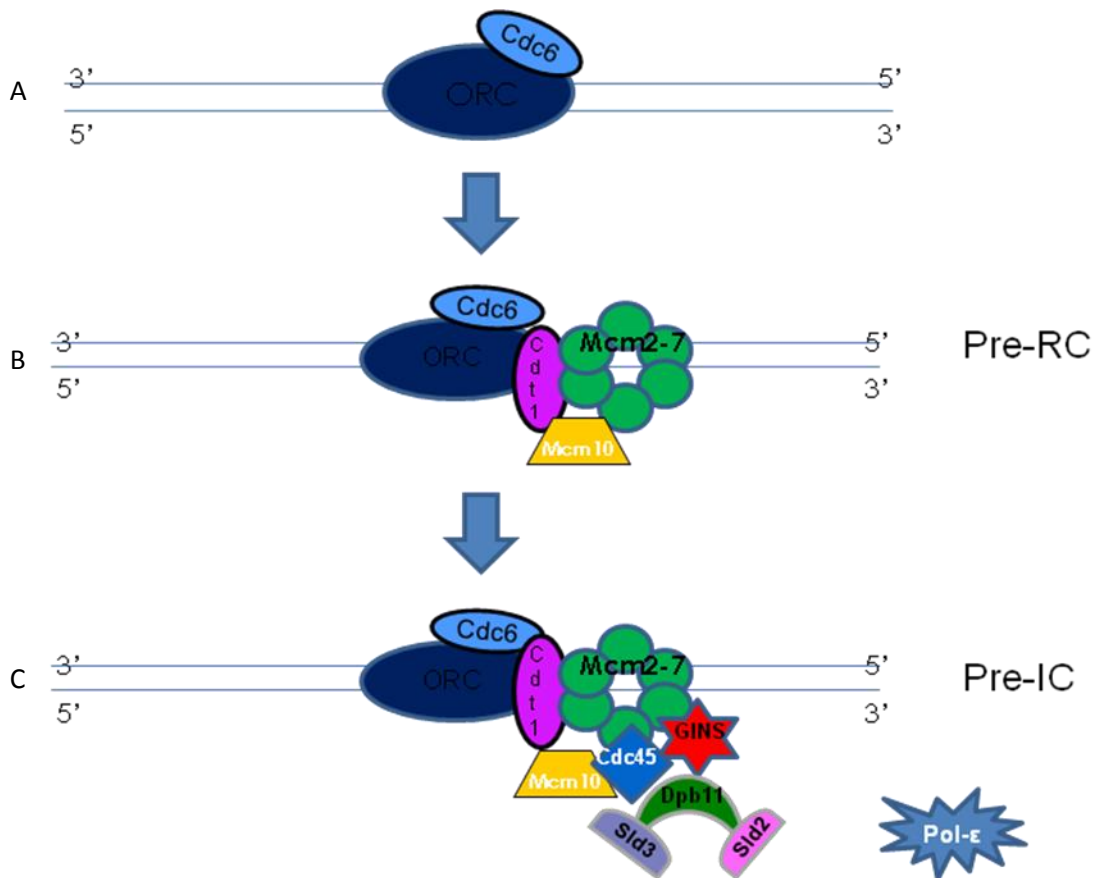


**Figure 2. Replication Initiation Complex Formation** A) ORC and Cdc6 bind to the origin to trigger recruitment of other replication proteins. B) Cdt1 loads Mcm2-7 onto the origin, allowing for the binding of Mcm10 and the completion of the Pre-RC. C) GINS and Cdc45 are recruited to the origin and bind to Mcm2-7, allowing for the association of over 20 other replication proteins, the completion of the Pre-IC and the G1/S phase transition.

The formation of the Pre-RC marks the licensing, or sufficient loading of the Mcm2-7 helicase complex for completion of replication only once, of the origin, and precedes the recruitment of multiple other replication proteins (6). Cyclin dependent kinases (CDKs) and Dpb4 dependent kinases (DDKs) are constantly present in the nucleus of the cell to regulate cycle progression. Specific CDKs and DDKs are responsible for the phosphorylation of different proteins throughout the process of replication (7, 8).

After formation of the Pre-RC, Cdc45 is recruited to the origin following phosphorylation of the Mcm2-7 complex by the Cdc7-Dbf4 complex (9, 6, 11). These two events happen in synchrony, and are immediately followed by the recruitment of the GINS complex which is facilitated by Mcm10 (12). The GINS complex is essential for the progression of DNA replication, and is predicted to increase the helicase activity of the Mcm2-7 proteins (13). After the recruitment of these proteins, the pre-Initiation Complex (Pre-IC) has formed, and the polymerases are recruited to complete the Replisome Progression Complex (RPC) (Figure 2c) (14). In order to efficiently replicate the entire genome, two pre-ICs are formed at the origin, allowing replication to proceed in a bidirectional and semiconservative fashion (6).

Following accurate and complete replication of the genome, the cell continues into G2 phase or the second growth phase of the cycle where the cell prepares for cytokinesis. At the G2 to M phase transition, Cdc25 is activated, and the cell transitions into mitosis (15). During mitosis, the chromosomes in the nucleus condense, align along the metaphase plate, and sister chromatids separate to the poles of the cell in preparation for cytokinesis (Figure 1).

## **b. GINS Complex**

The GINS Complex, whose name is derived from the Japanese Go, Ichi, Ni, San for 5-1-2-3, is a highly conserved heterotetrameric complex composed of the subunits Sld5, Psf1, Psf2, and Psf3 (Figure 3) (1). Originally discovered in yeast, the GINS complex is required for both replication initiation and

elongation (13). Although GINS is shown to increase the helicase activity of the Mcm2-7 complex, it is also implicated in enhancing the polymerase activity of Pol- $\alpha$  and Pol- $\epsilon$  (1, 16). Through its interactions with Mcm2-7 and Cdc45, GINS is a member of the Replisome Progression Complex that moves with the replication fork during elongation (9, 14). Each of the four subunits is required for the association of the complex, and the absence of one subunit leads to a stalled replication fork (17).

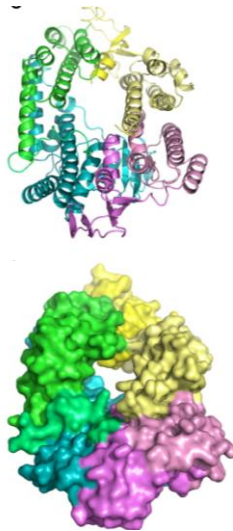


**Figure 3. Crystal Structure of the Human GINS Complex** (top) Alpha helices and beta sheets of each of the four subunits of GINS, arranged in the ring structure. (bottom) Surface representation of the ring shaped complex. Purple=Psf2, Blue=Sld5, Green=Psf1, Yellow=Psf1 (18)

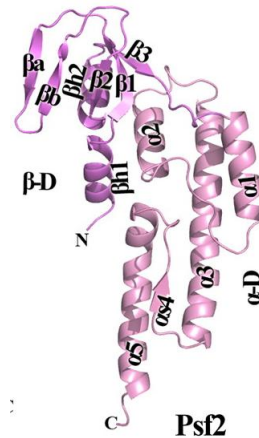


**Figure 4.** Crystal structure of Psf2 (18).

The four subunits of the Complex are divided into pairs based on their structural similarity: Psf1-Sld5 and Psf2-Psf3. Each subunit consists of multiple alpha helices responsible for the interactions between subunits, followed by intermittent beta sheets hypothesized to interact with other replication proteins (17). The essential function of the GINS Complex is highly conserved and GINS homologues have been identified in Archea as well. In addition to interacting with the MCM proteins, the Archaeal GINS complex also shares many structural similarities to the eukaryotic GINS complex (19). Although archeal GINS is composed of only two subunits, GINS 23 and GINS 15, the structural similarity of each of

the archeal subunits mirrors that of the eukaryotic subunits that are paired based on structural similarity: Psf2-Psf3 and Psf1-Sld5 respectively (19).

Psf2 (Partner of Sld-five 2) has been shown to interact with Sld5 and Psf3 in forming the ring-shaped structure of the GINS complex (Figure 4) (21). In addition to its role within the Complex in DNA replication, Psf2 has also been implicated in chromosome segregation during M phase of the cell cycle in *S. pombe* and human tissue cultures (4). Additionally, levels of Psf2 have been shown to be upregulated in liver cancer cells, and Psf2 is shown to interact with Chk2, a DNA damage and a G2-M checkpoint protein, in humans (22, 23, 24). Finally, Psf2 has demonstrated a tissue specific role affecting eye development in *Xenopus* (25). Despite the previous research on Psf2, there are still many remaining questions into the function of Psf2. Primarily, previous research has formed a connection between many of these other defects, without specifically studying the function of the protein itself. Additionally, all of the previous research in eukaryotes has been performed *in vitro* as opposed to *in vivo*.

In order to further characterize the role of Psf2 we utilized a homozygous lethal mutant in *Drosophila melanogaster*. Utilizing a p-element insertion into the *psf2* allele leading to a 61 amino acid truncation of the protein could provide insight into the role of *psf2 in vivo*. Additionally, this C-terminal truncation removes the last, highly conserved, alpha helical domain responsible for the Psf2-Psf3 interaction during GINS complex formation (Figure 5) (19). Since each subunit is essential for proper formation of the GINS Complex, it is hypothesized that this C-terminal truncation would lead to malformation and inactivation of the GINS complex. *Drosophila* has already been established as a model organism for higher eukaryotes (26). Additionally, *Drosophila* has a fully sequenced genome and a vast availability of tools and techniques, making it an ideal organism for use as a research tool. In addition to observation of phenotypes in varying tissues in a mutant *psf2* fly, we also are utilizing yeast two hybrid

analysis to provide insight into the role of Psf2 throughout DNA replication and elsewhere in the cell cycle.

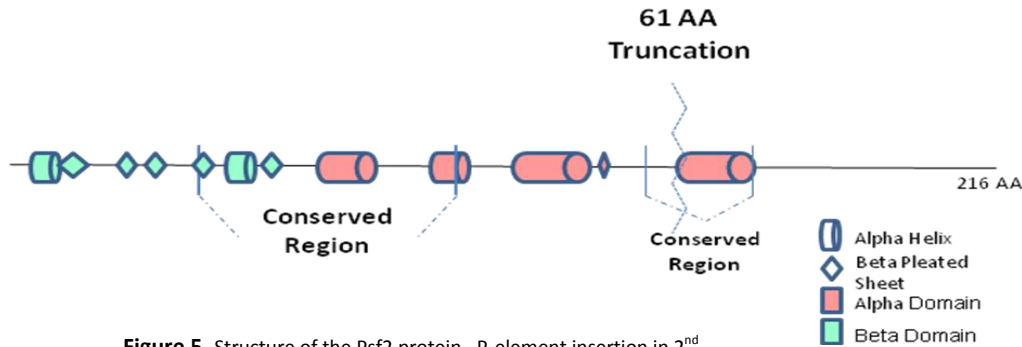


**Figure 5.** Structure of the Psf2 protein. P-element insertion in 2<sup>nd</sup> conserved region leads to 61 AA truncation and removal of the last alpha helical region

## II. Specific Aims

Defects in the assembly and progression of the replication machinery provide the basis for many disease states, specifically, cancer (21). Additionally, many of these proteins have separable roles throughout the cell cycle in tissue differentiation, cell cycle checkpoints, and chromatin dynamics (11, 21). Increasing our knowledge of the role of these replication proteins throughout the cell cycle could prove beneficial in the treatment of many diseases.

The characterization of *psf2* will likely provide insight into its specific role within the GINS complex and elsewhere in the cell. I utilized *Drosophila melanogaster* as a model organism to address the following hypothesis regarding GINS and Psf2:

**The *Drosophila* Psf2 protein plays a role in DNA replication.**

I addressed this hypothesis through the following specific aims:

**Specific aim #1: Characterize mutant *psf2* phenotype**

In order to test the role of *Drosophila* Psf2 throughout the cell cycle, I utilized a homozygous lethal *psf2* mutation to observe phenotypes within multiple tissues. First, observation of the larval brain tissue provided insight into the role of *psf2* in normal cycling cells. Second, observation of the larval salivary tissue and ovarioles allowed for the assessment of a possible role for *psf2* in endoreplicating tissue. Finally, observation of *Drosophila* embryos allowed for detection of defects in cell cycle progression and chromatin dynamics.

### **Specific aim #2: Identify interactions between *psf2* and other replication proteins**

Psf2 has been previously implicated as a member of the GINS Complex which associates with the pre-RC during DNA replication initiation. The exact mechanism of the recruitment and association of these proteins is still unknown. Using the yeast two-hybrid system, I tested for interactions between Psf2 and other replication proteins in *Drosophila*.

### **Specific aim #3: Deplete levels of *psf2* and observe phenotypes**

The *psf2* mutant fly contains a p-element insertion truncating the last 61 amino acids. In addition to observing the phenotypes in this truncated mutant, I utilized RNAi knockdown using the Gal4-UAS system to deplete levels of Psf2 in different tissues and observe the phenotypes.

## **III. Materials and Methods**

**Genomic DNA extraction:** First, 30 wildtype anesthetized flies were placed in a 1.5 mL Eppendorf tube (Fisher™) and stored at -80°C. When ready for the extraction, 200 µL Buffer A (Table 1) was added and tissue was ground using a disposable tissue grinder. Then, 200 µL additional Buffer A was added, and flies were ground until only cuticles remained. Next, samples were incubated at 65°C for 30 minutes. After 30 minutes, 800 µL Buffer B (Table 2) was added, mixed by inverting the tube and incubated for 1

hour on ice. Next, samples were centrifuged at 12,000 rpm for 15 minutes at room temperature. The supernatant was then transferred into a new 1.5 mL Eppendorf tube, and 600  $\mu$ L isopropanol was added to each sample and mixed. The sample was then centrifuged at 12,000 rpm for 15 minutes at room temperature. Next, the supernatant was discarded, and the pellet was washed with 70% ethanol. The majority of the ethanol was removed with a p200 pipette, and the sample was allowed to air dry until all the ethanol was removed. Genomic DNA was resuspended using dH<sub>2</sub>O and stored at -20°C.

Component	Concentration
Tris-Cl (pH 7.5)	100 mM
EDTA	100 mM
NaCl	100 mM
SDS	0.5%

Table 1. Components of Buffer A stored at room temperature.

Component	Amount Added
5 M Potassium Acetate	200 mL
6 M Lithium Chloride	500 mL

Table 2. Components of Buffer B stored at 4°C.

**PCR:** Psf2 cDNA was amplified using Platinum Pfx DNA polymerase (Invitrogen™). Amounts added can be seen in Table 3. To start, components were denatured at 94°C for 2 minutes followed by 35 cycles each with 15 seconds of denaturation at 94°C, annealing at 57°C for 30 seconds and a 1 minute

extension time. Primers used are displayed in Table 4. Genomic DNA was amplified using *psf2* 2000+ genomic topo and *psf2* minus stop (Integrated DNA Technologies™), and cDNA was amplified using *psf2* plus stop codon and *psf2* start topo (Integrated DNA Technologies™). PCR products were tested with gel electrophoresis in a 1% agarose gel run at 135 V for 30 minutes.

Component (Invitrogen™)	Amount Added ( $\mu$ L)
5X Pfx Amplification Buffer	5
Primers (10 $\mu$ M )	1.5 of each
dNTP (10 $\mu$ M)	1.5
MgSO <sub>4</sub> (10mM)	1
Psf2 CDNA	1
Platinum Pfx	1
dH <sub>2</sub> O	To 50 $\mu$ L

Table 3. Components added for PCR

Primer Name (Integrated DNA Technologies™)	Sequence 5'—3'
Psf2 Start topo	CACCATGTTCCCGCATTTGTTTTG
Psf2 plus stop codon	TCACTGAGAAAACAGAGAGTTACTGTTC

Psf2 2000+ genomic promo topo	CACCCGTATATAGTTTAAAATTGAGATCACTTTTG
Psf2 minus stop codon	CTGAGAAAACAGAGAGTTACTGTTCGG

Table 4. Primers used to amplify Psf2

**Cloning Psf2 into Plasmids:** After confirming the size of the PCR product, the insert was first cloned in the pENTr-d-TOPO entry vector (Invitrogen™). Amounts added to 1.5 mL Eppendorf tube are displayed in Table 5. The Cocktail was incubated for 5 minutes at 25°C, followed by the addition of 50µL competent *e.coli* cells to the vector mixture and placed on ice for 30 minutes. Next, cells were heat shocked for 30 seconds at 42°C, followed by the addition of 100µL LB broth and a 45 minute incubation period at 37°C. After incubation, cells were plated on LB media supplemented with kanamycin to select for the p-ENTr-d-TOPO vector (Invitrogen™) and incubated overnight at 37°C. After 14-24 hours, colonies were selected and grown in LB broth overnight. DNA was isolated using Minipreps™ (Promega™) and sequenced to confirm cloning of insert into the entry vector.

After sequencing, the insert was cloned from the entry vector to one of three destination vectors: pGAD T7, pGBK T7 or pTWF using LR Clonase (Invitrogen™). Amounts added to 1.5mL Eppendorf tube are displayed in Table 6. The Cocktail was incubated for 1 hour at room temperature, followed by transformation into *e.coli* as seen above. The Reaction was plated on LB media supplemented with ampicillin to select for the pGBK (Clonotech™), pGAD (Clonotech™), and pTWF (Murphy™) vectors followed by incubation overnight at 37°C. After 14-24 hours, colonies were selected and grown in LB broth overnight. DNA was isolated using Minipreps™ (Promega™) and sequenced to confirm cloning on insert into the destination vectors.

Component	Amount Added ( $\mu\text{L}$ )
PCR Product	2
p-ENTR-d-TOPO salt solution (Invitrogen™)	1
p-ENTR-d-TOPO vector enzyme (Invitrogen™)	1
dH <sub>2</sub> O	2

Table 5. Components added for entry vector cloning

Component	Amount Added ( $\mu\text{L}$ )
p-ENTR-d-TOPO vector containing insert	3
Destination vector (pGADT7, pGBKT7, pTWF)	3
LR Clonase enzyme (Vortexed) (Invitrogen™)	2
LR Clonase Buffer (Invitrogen™)	3

Table 6. Components added for destination vector cloning.

**Transgenic Fly Cross:** First, genomic Psf2 was cloned into the pTWF (Murphy™) vector using LR clonase reaction seen above. The resulting vector with Psf2 cloned into the gateway cassette was mailed to Best Gene Inc. for generation of the transgenic fly as seen in Figure 6. Balancer chromosomes, depicted as CyO, Gla, and sb, are essential for preventing homologous recombination, and persistence of a true breeding stock. These balancer chromosomes are recessive lethal, allowing for the persistence of the heterozygous mutation. Additionally, the balancer chromosome contains multiple inversions to prevent

recombination during cross over events. This allows for the persistence of the true breeding, heterozygous stock.

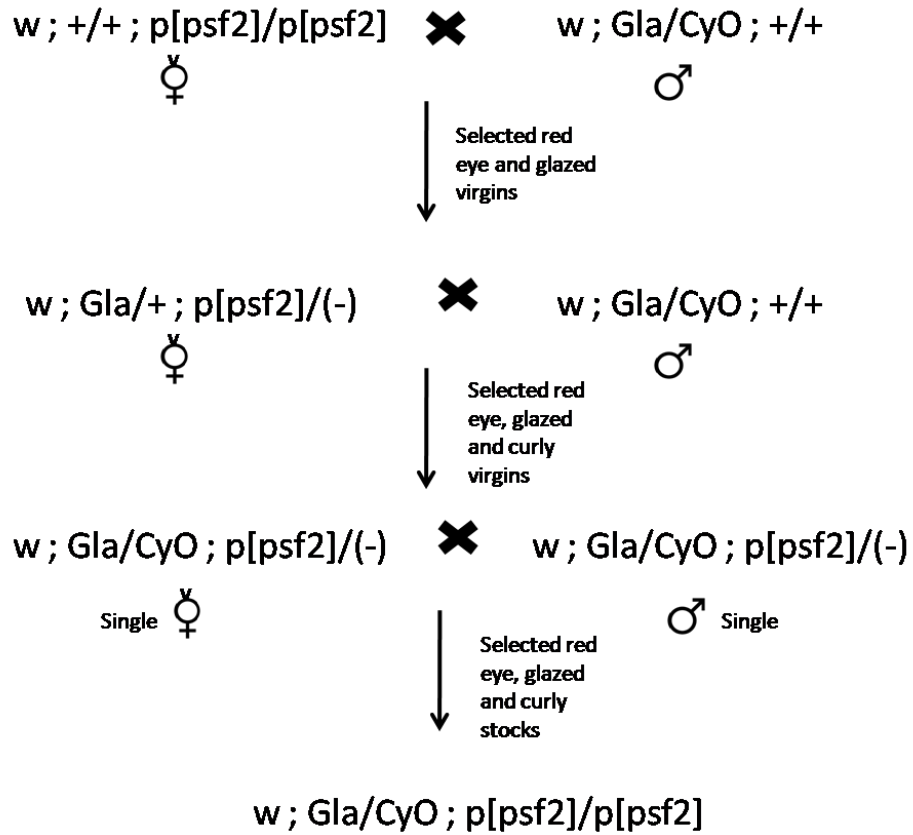


Figure 6. Generation of transgenic fly

In stocks with persisting red eyes, the following cross was completed and stocks were monitored to see if the CyO wing phenotype was lost (Figure 7).

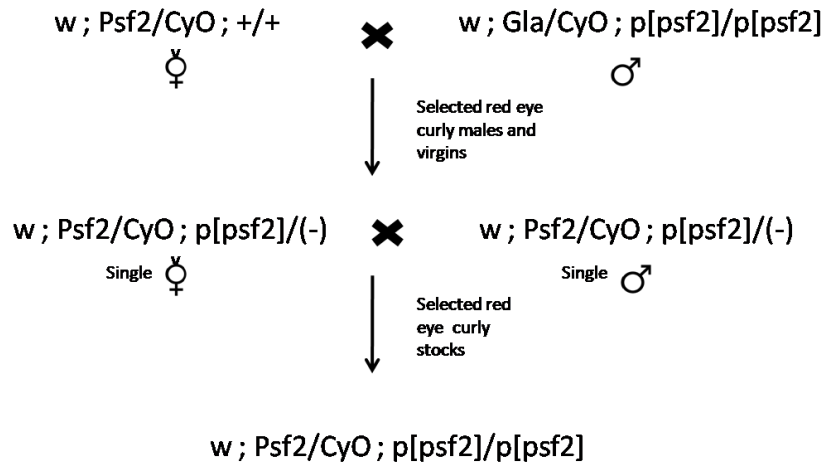


Figure 7. Generation of rescue fly

**Homozygous Mutant Fly Cross:** Generation of the homozygous *Psf2* fly was performed as seen in Figure

8.

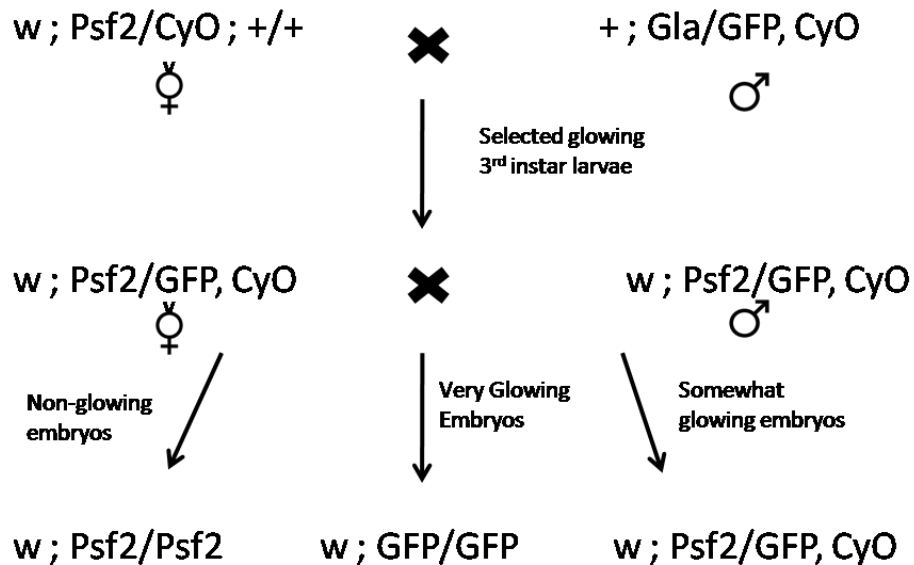


Figure 8. Generation of homozygous mutants

*w ; Psf2/GFP, CyO* females were fed with yeast paste overnight, followed by embryo collection on grape agar plates. After 6 hours, embryos were observed under a dissecting microscope with UV filter where non glowing embryos (*psf2/psf2*) were selected and placed on a grid on grape agar (Genesee Scientific™)

plates for observation. Additionally, slightly glowing embryos were also collected and placed in a grid on grape agar plates for observation to act as a control.

**Polytene Chromosomes:** 3<sup>rd</sup> instar wandering larvae were isolated and placed in a dual concavity slide with 50  $\mu$ L 1X PBS pH 7.2 with 1% PEG 8000 in one well. Salivary glands were dissected out using Dumoxel™ Tweezers #5 (Electron Microscopy Sciences™) and moved to the second well into a solution of 50% acetic acid, 2-3% lactic acid, 3.7% formaldehyde and fixed for 2 minutes. Salivary glands were then transferred using a p20 pipette to a cleaned microscope slide where they were covered with a siliconized coverslip (coverslips prepared by dipping into Sigmacote™ (Sigma™)). Next, a piece of filter paper was placed on top of the slide, and the salivary tissue was spread using a circular tapping motion with a pencil for 2 minutes. Once spread, a piece of filter paper was sandwiched between the spread salivary tissue and a clean microscope slide, and placed in a machinist vice. Pressure was applied using a torque wrench to 15 nM for 2 minutes. The slide was then removed from the vice, and placed in liquid nitrogen for 1 minute. The siliconized coverslip was removed using a razorblade, and the slide was placed in ethanol for 30 seconds. After 30 seconds, the slide was removed from the ethanol and placed in a centrifuge to air dry. Once dry, the slide was stained and mounted with 7mL of Vectashield™ (Vector™) with DAPI and stored at 4°C.

**Embryo Collection and microscopy:** Female fly stocks were isolated and fed overnight with a yeast paste made from 1:1 mixture of active dry yeast and dH<sub>2</sub>O overnight followed by embryo collection on grape agar plates. After 5 hours, embryos were collected on the grape agar plate using dH<sub>2</sub>O and a paintbrush. The embryos were removed from the grape plate using a p1000 pipette and placed in a mesh basket. The mesh basket was made by cutting the bottom off of a 2 mL cryogenic tube and placing a piece fine mesh over the top. Next, the mesh basket was placed under a dissecting microscope, and a 50% bleach solution in dH<sub>2</sub>O was pipetted into the mesh basket, while monitoring the embryos through the

dissecting microscope for removal of the chorion by the 50% bleach solution. Once the dorsal appendages disappeared from the posterior of the embryos, the embryos were then washed with an Embryo solution (7% NaCl, 0.5% Triton X-100, dH<sub>2</sub>O) followed by washing with dH<sub>2</sub>O. Next, embryos were transferred to 5mL glass vials where they were washed off of the mesh using 1 mL of Heptane. Next, 1 mL of Methanol was added to the vial, followed by 25 seconds of vigorous shaking to devitalize the embryos. After all the embryos settled to the bottom of the vial, the upper Heptane layer was removed, and embryos were stored in Methanol at 4°C if desired. After optional storage, the methanol was removed, and embryos were rehydrated with PBTA (1X PBS, 1% BSA, 0.02% Sodium Azide, 0.05% Triton X-100) for 15 minutes on a rotator. Next, embryonic DNA was stained with a 1µg/mL DAPI solution in PBTA at room temperature for 5 minutes in the dark. Following 3X 5 minute washes and 1 hour wash with PBTA, embryos were mounted using two Lifterslip™ (Thermo Scientific™) slides using Vectashield™ (Vector™) and imaged. Microscopy was performed using an Olympus IX81 Motorized Inverted Microscope with Spinning Disk Confocal, and images were analyzed using Slidebook™ software.

**Brain Squashes/Mitotic Indices:** 3<sup>rd</sup> instar wandering larvae were isolated and placed in a dual concavity well with one side filled with 1X PBS pH7.2 with 1% PEG 8000. Brains were dissected out and moved to the second well and placed in a hypotonic solution of 0.5% Sodium Citrate for 10 minutes. The larval brains were then transferred to a clean microscope slide using a p20 pipette, and covered with a siliconized coverslip (generated by dipping a glass coverslip into Sigmacote™ (Sigma™)). The brain was carefully sandwiched between the cleaned slide, filter paper and a second slide, placed in the machinist vice with 15 nM of pressure applied using a torque wrench. After 2 minutes, the slide was removed and placed in liquid nitrogen for 1 minute. The siliconized coverslip was removed using a razorblade, and the slide was placed in ethanol for 30 seconds. After removing from the ethanol, the slide was placed in a centrifuge to air dry. Once dry, the brain was mounted with 7mL of Vectashield™ (Vector™) with DAPI and stored at 4°C.

Mitotic indices were performed by selecting 10 well populated random fields of view for each brain squash and imaged using 60X magnification on the Olympus IX81 Motorized Inverted Microscope with Spinning Disk Confocal. The total number of nuclei were counted for each field of view and divided by the number of mitotic figures per the same field of view. Statistical analysis was performed using Minitab™ Statistical Software.

**Antibody Staining:** Embryos were collected using the protocol above for embryo collection. However, the embryos were extracted from the grape plates (Genesee Scientific™) after 10 hours, as opposed to 5 hours. The longer collection time allowed embryos to develop past the early embryo stage into the late stages of embryonic development. After rehydrating with PBTA for 15 minutes on a rotator, embryos were stained with 1µg/ml rabbit antibody to phosphor H3 (Millipore™) and incubated at room temperature on a rotator for 5 hours. Following the 5 hours, the embryos were washed 3X with PBTA, and placed on the rotator in 4°C overnight in PBTA. Next, the embryos were stained with 1 µg/ml of Anti-Rabbit antibody to phospho H3 conjugated to a fluorescein (Millipore™) and incubated for one hour in the dark at room temperature on a rotator. Embryos were then washed 3X in PBTA followed by a 1 hour wash in PBTA. Next, DNA was stained using a 1µg/mL DAPI solution in PBTA for 5 minutes, followed by 3X 10 minute washes and a 1 hour wash in PBTA. Embryos were moved to a clean a Liftaslide®(Thermo Scientific™) and mounted using Vectashield® (Vector™). Microscopy was performed using a Olympus IX81 Motorized Inverted Microscope with Spinning Disk Confocal using GFP and DAPI filters followed by analysis using Slidebook™ software.

**Ovary/Follicle Dissection and Imaging:** Female fly stocks 3-7 days post eclosion were fed for 2 days with a 1:1 mixture of active dry yeast and dH<sub>2</sub>O. Random female flies were selected, and ovaries were dissected out in a dual concavity slide in one well with 50 µL 1X PBS. Ovarioles were teased apart using a needlepoint tool, moved to the second well, and fixed for 20 minutes in a 4% Formaldehyde in PBX (PBS

with 1% Triton X-100). After fixing, ovaries were moved to a new well and stained for 5 minutes in a 1 µg/ml DAPI in PBS. Ovaries were then washed 3X in PBX, followed by a 1 hour PBX wash, and 3X 10 minute washes in PBX. Ovaries were then moved using Dumoxel™ Tweezers #5 (Electron Microscopy Sciences™) to a clean Lifterslip™ (Thermo Scientific™), mounted with Vectashield™ (Vector™) and imaged using confocal optical sectioning microscopy.

**EdU incorporation assays:** 3<sup>rd</sup> instar wandering larvae were isolated and placed in a dual concavity slide in Grace's cell culture solution, and brains were removed from the larvae and cleaned using Dumoxel™ Tweezers #5 (Electron Microscopy Sciences™). An equal volume of 200 mM of the Click-it EdU reaction solution (Invitrogen™) in DMSO was added to the well and brains were incubated in the dark at room temperature for 30 minutes. Following incubation, the liquid was removed from the well using a p200 pipette and the brains were washed 2X with 1X PBS. The 1X PBS was then removed, and brains were fixed in 3.7% Formaldehyde solution in PBS for 15 minutes followed by 2X washes in 1X PBS. Next, brains were permeabilized using 0.1% Triton-X in PBS for 15 minutes. Brains were then incubated for 30 minutes in the Click it® Reaction (Invitrogen™) cocktail followed by 2 washes with the reaction buffer per manufacturer's instructions. The rinse buffer was removed and brains were stained using 0.1% Hoescht 33342 in dH<sub>2</sub>O for 18 minutes. The stain was removed from the well and brains were washed 2X using PBS. Brains were then mounted on a clean Lifterslip™ (Thermo Scientific™) using Vectashield™ (Vector™). Imaging was completed using the Olympus IX81 Motorized Inverted Microscope with Spinning Disk Confocal using GFP and DAPI filters.

**Yeast Two-Hybrid Analysis:** Protocol performed as from Apger et. Al. (41).

## Chapter 2: Results

### IV. Results

## **Psf2 homozygous mutant arrest in M phase during the late embryo/1<sup>st</sup> instar larval developmental stage**

In order to confirm the p-element insertion in the *psf2* mutant fly line produced inviable homozygous offspring, *psf2* mutant fly strains were crossed to a GFP tagged fly line. *Psf/CyO, GFP* larvae were isolated as a true-breeding stock. Female *psf2/CyO, GFP* adult flies were fed with yeast paste overnight, and embryos were collected on grape agar plates for analysis. Twenty five embryos from *psf2/psf2* embryos (non-glowing embryos) and wildtype embryos were placed in a grid formation. After 48 hours, all of the wildtype embryos hatched and developed into 2<sup>nd</sup> instar larvae, while only two of the *psf2/psf2* embryos hatched. Of those that hatched, all of the 1<sup>st</sup> instar larvae arrested immediately. Therefore, we confirmed the homozygous lethality of the *psf2* mutant fly, and determined the arrest point at the late embryo/1<sup>st</sup> instar larval transition.

## **Psf2/Psf2 arrests in M phase of the cell cycle**

After determining the late embryonic arrest point, homozygous *psf2* embryos were collected to determine the phase of the cell cycle in which they arrested. Mutant and wildtype embryos were stained with a rabbit antibody to phosphoH3. A secondary anti-rabbit antibody conjugated with a fluorescein was added for detection of M phase cells and DAPI to stain DNA. After imaging, *psf2* homozygous mutant embryos displayed more cells in M phase, confirming an M phase arrest point in late embryonic development (Figure 9).

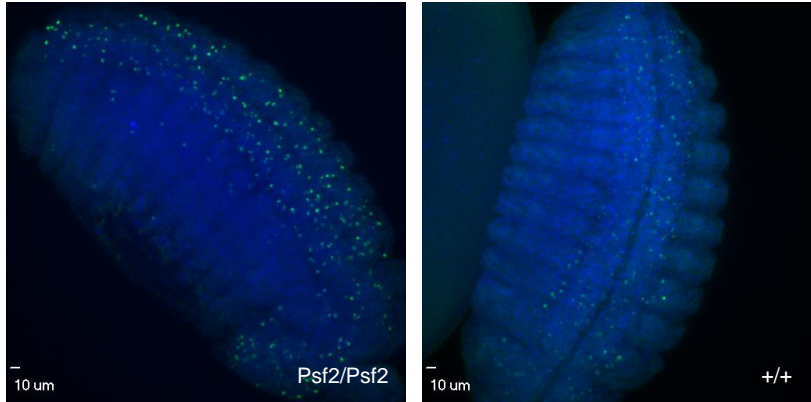


**Figure 9. Homozygous Mutant Late Embryonic Arrest Visualization.** *Psf2* homozygous mutant embryos were collected and stained with antibody to phosphor H3 identifying cells in M phase (green). Additionally, embryos were stained with DAPI (blue) to identify cells in interphase. Observation of 10 hour embryos shows increased cells in M phase in *psf2/psf2* (left) versus wildtype (right).

### Flies heterozygous for the *psf2* mutation display M phase delay in 3<sup>rd</sup> instar larval brain tissue

Since the *psf2* homozygous mutant arrests in M phase, we wanted to examine the cell cycle progression of the normal cycling larval brain tissue. Wildtype and *psf2/CyO* mutant 3<sup>rd</sup> instar wandering larval brains were dissected and stained with DAPI for analysis. An average mitotic index for wildtype larval brains was 0.37% while an average mitotic index for *psf2* heterozygous mutant was 2.4%. T-test analysis indicates a statistically significant difference between mitotic indices of wildtype and mutant flies with a p-value of 0.004 (Figure 10).

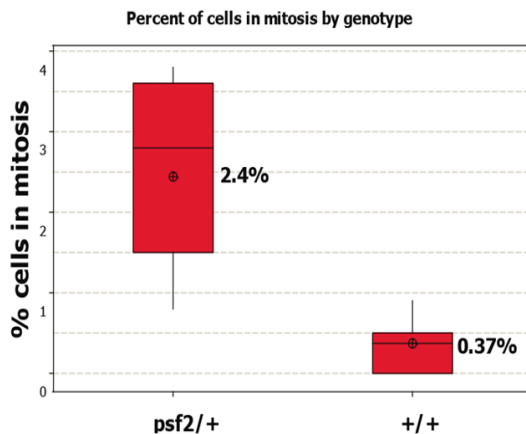


**Figure 10. Mitotic Index for Psf2 Heterozygous Mutant.** Wildtype and *psf2/+* 3<sup>rd</sup> instar wandering larval brains were dissected and squashed for observation. The number of mitotic figures were counted and divided by the number of cells in interphase to calculate the mitotic index. *Psf2/+* larval brains (left) displayed a mitotic index significantly higher than that of wildtype.

## **Psf2 heterozygous mutant displays increased aneuploidy and defects in chromosome dynamics in 3<sup>rd</sup> instar larval brain tissue**

Previously, *psf2* has been implicated in chromatin segregation during M phase (4). Therefore, we examined the mutant's mitotic figures in the larval brain tissue compared to wildtype. The *psf2/CyO* mutant displayed more aneuploid cells (Figure 11a) compared to wildtype, along with defects in chromosome dynamics, such as arm length and broken chromosomes (Figure 11b).

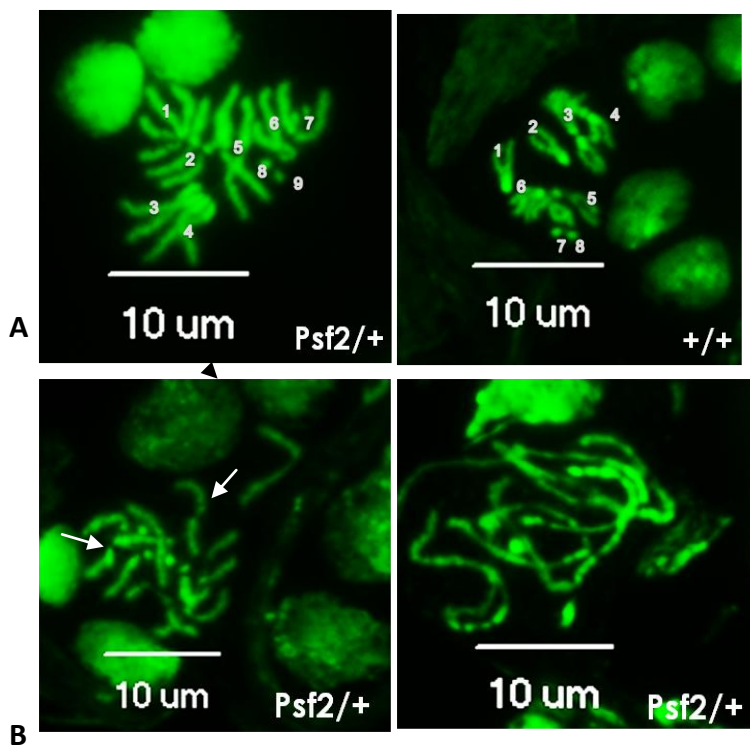


**Figure 11. Defects Chromosome Dynamics Visualized in Larval Brains** A) *psf2/+* displays an increase in aneuploid cells (left). Wildtype *Drosophila* brains display the correct number, 8, chromosomes (right). B) *Psf2/+* mutant displays defects in chromosome dynamics. Many of the chromosomes displayed broken arms (see arrows on left), along with condensations defects (see bottom right).

## **Psf2 heterozygous mutant displays an M phase delay visible using EdU S phase staining**

After observing an M phase delay, we wanted to confirm a role for *psf2* in either M or S phase of the cell cycle. Therefore, we incorporated an azide tagged thymidine analogue (EdU) into 3<sup>rd</sup> instar larval brain tissue to indicate cells undergoing DNA replication. The *psf2/CyO* mutant shows fewer cells

incorporating the EdU molecule into the genome, confirming the M phase delay in larval brain tissue (Figure 12).

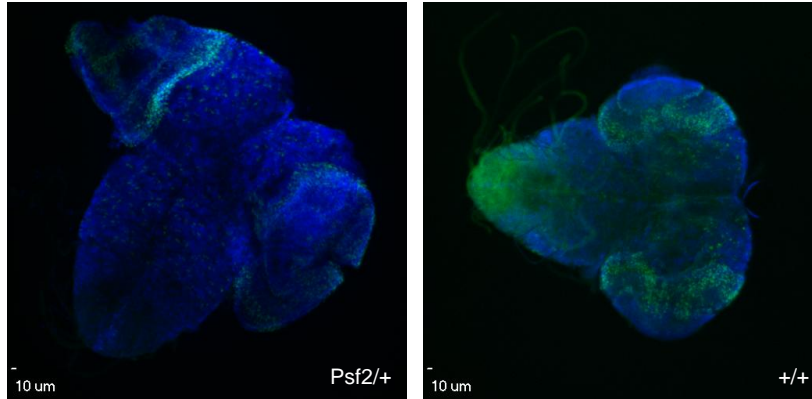


**Figure 12. EdU Incorporation in *psf2* Heterozygous Larval Brains.** *Psf2*<sup>+/+</sup> displays M phase delay visible in 3<sup>rd</sup> instar wandering larval brains. Use of EdU to incorporate an azide tagged thymidine analogue to image cells in S phase (green), to compare DAPI stained cells elsewhere in the cell cycle (blue). *Psf2*<sup>+/+</sup> mutant displays less cells incorporating the EdU compared to wildtype, confirming the M phase delay.

### ***Psf2* mutant displays defects in cell cycle progression and chromatin dynamics visible in early embryos**

*Drosophila* early embryo cell cycles occur in a syncytium with few checkpoint controls (28). Since the *psf2* mutant displays an M phase delay, we wanted to observe the progression of the cell cycle with little inhibition by checkpoint controls. Homozygous mutant *psf2* and wildtype 5 hour embryos were collected on grape agar plates and stained with DAPI. After imaging, wildtype embryos nuclei appear synchronized in one phase of the cycle, while *psf2* mutant embryos display multiple nuclei in each phase of the cell cycle (Figure 13a). In addition to the asynchrony of nuclei in the *psf2* mutant, wildtype embryos displayed a uniform distribution of cells, while the *psf2* mutant displayed multiple gaps where cells died, and dropped out of the periphery (Figure 13b).

Additionally, the migration of the nuclei to the periphery allows for easy examination of the chromatin dynamics of the nuclei progressing through M phase. Therefore, we closely examined the mitotic figures of both the *psf2* mutant and wildtype nuclei to confirm any defects in mitosis. Upon

examination, *psf2* mutant chromosomes formed anaphase bridges (Figure 13c).

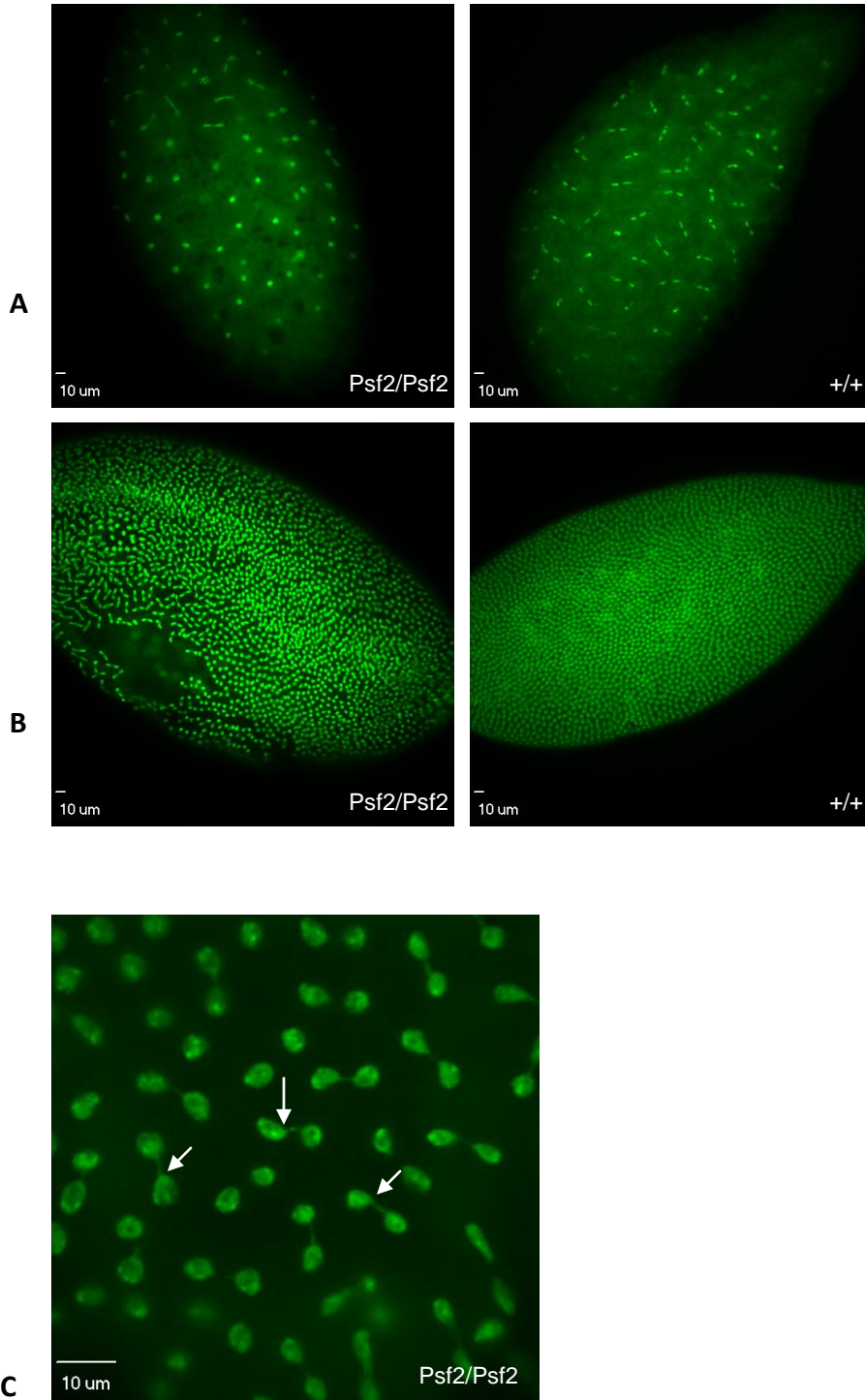


**Figure 13. Defects Visualized in Homozygous *psf2* Early Embryos.** a) *Psf2/psf2* embryos displays asynchrony in the syncytial cell cycle (left). b) Wildtype embryos (right) display a uniform distribution of cells in the periphery while *psf2/psf2* embryos do not have a uniform distribution with cells dropping out of the periphery (left). c) *Psf2/psf2* embryos display anaphase bridges.

### **Psf2 mutant fly displays defects in DNA replication in endocycling tissues**

Psf2 is one of four subunits in the GINS complex, which plays a role in enhancing helicase activity of the Mcm2-7 complex during DNA replication, initiation, and elongation (13). Additionally, knockdown of *psf2* has been previously shown to lead to stalled replication forks and a decrease in replication of the genome (4). Therefore, we wanted to test the *psf2/Cyo* mutant fly for defects in DNA replication. To do this, we examined the polytene salivary tissue of the 3<sup>rd</sup> instar wandering larvae in wildtype and *psf2* stocks. Endocycling tissues display a unique cell cycle with one growth phase, G, followed by a normal S phase of the cycle and no subsequent cytokinesis (29). Endocycling tissues, or polytene tissues, are polyploid and contain highly banded chromosomes containing small amounts of heterochromatin, and are easily visualized for gene localization (29). Since *psf2* is hypothesized to play a role in replication, examination of the endocycling tissues, which only go through S phase and G phase, could provide insight into the role of *psf2* within the cell cycle (29). Salivary tissue was removed from the larvae and stained with DAPI for analysis. Compared to wildtype, *psf2* heterozygous mutants displayed smaller polytene chromosomes, indicating a defect in DNA replication in endoreplicating tissue (Figure 14).

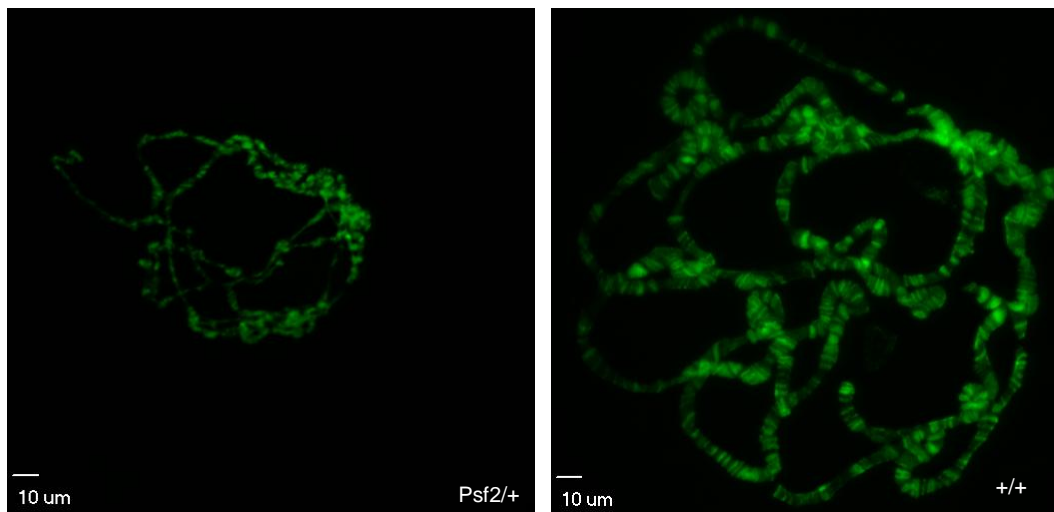
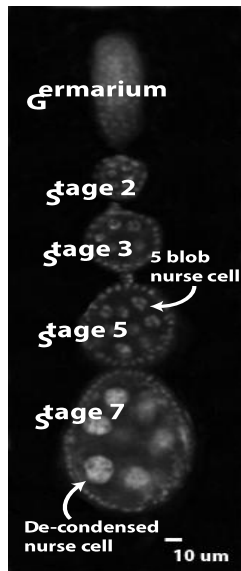


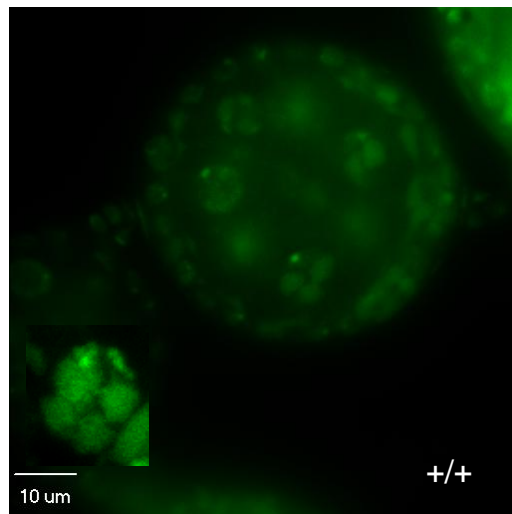
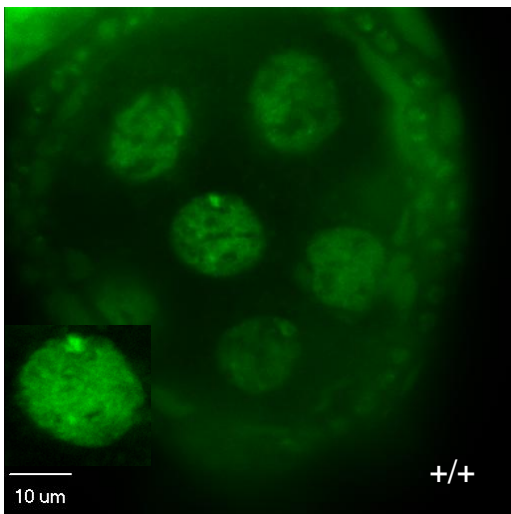
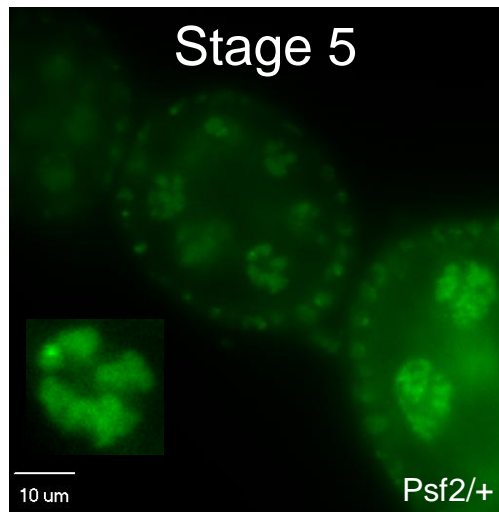
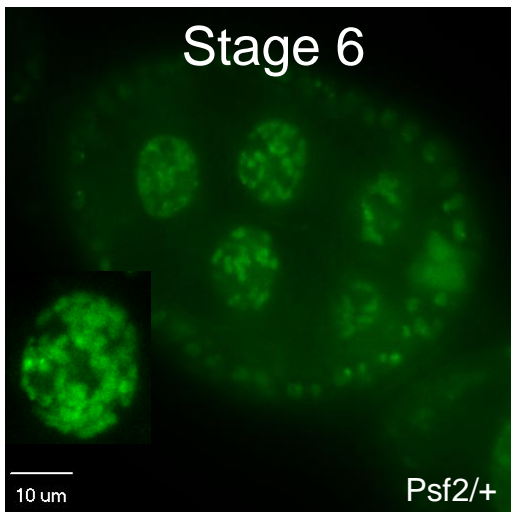
**Figure 14. Heterozygous *psf2* Mutants Display Defects in Salivary Tissue.** *psf2/+* 3<sup>rd</sup> instar wandering larval salivary tissue displays smaller polytene chromosomes (left) compared to wildtype salivary tissue (right).

Previous data implicates *psf2* in chromosome segregation and interaction with other proteins involved in chromosome dynamics (4). Since our *in vivo* observation also implicated *psf2* playing a crucial role in the endoreplicating salivary glands, we also wanted to analyze the nurse cells within the ovarioles which are also endoreplicating tissue. Female wildtype and heterozygous *psf2* mutant flies were fed yeast paste overnight for 2 days, and random females were selected for dissection of their ovaries. Ovarioles were teased apart and fixed, followed by staining with DAPI. After imaging, the *psf2* mutant nurse cells displayed varying chromosome size, indicating a defect in DNA replication (Figure 15c).

Additionally, nurse cell chromosomes undergo multiple stages with varying chromosome characteristics. During stage 4 of development, nurse cell chromosome persists in a polytene state, similar to those seen in the salivary glands. At stage 5, the chromosomes condense into a characteristic “5 blob” stage, followed by decondensing of the chromosomes at stage 6 (Figure 15a) (30). Examination of the wildtype and *psf2/CyO* mutant ovaries show a defect in the progression of chromosome from condensed state at stage 5 to the decondensed state at stage 6 (Figure 15b). Chromosomes in the *psf2/CyO* mutant appear less condensed, similar to the polytene state of stage 4, suggesting a role for *psf2* in decondensation of the nurse cell chromosomes.



A



B

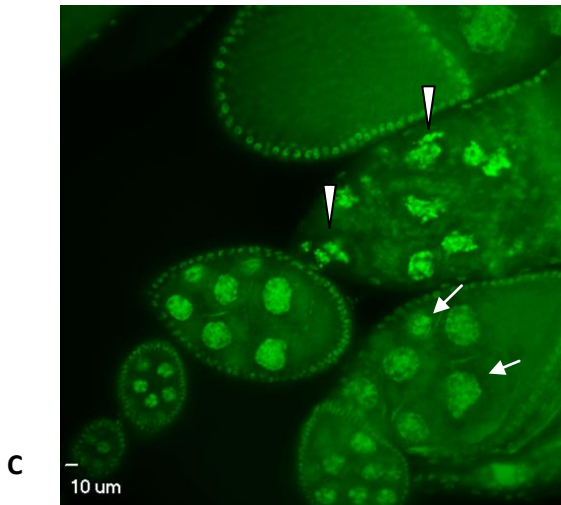


**Figure 15. *psf2* Heterozygous Mutants Display Defects in Ovariole Development.** a) Nurse cell chromosomes undergo condensation into a characteristic 5 blob appearance at stage 5, followed by decondensation in stage 6. b) *Psf2/CyO* female flies display normal polytene chromosomes in stage 3 of the developing nurse cell within the ovaries (data not shown). At stage 4, *psf2/CyO* displays a normal condensed “5 blob” stage compared to wildtype (right column). During stage 5, chromosomes decondense from the “5 blob” stage. *Psf2/CyO* female ovaries display defects in the condensation state, where they appear more polytene compared to wildtype (left column). c) *Psf2/CyO* nurse cells appear in various shapes and sizes indicating defects in DNA replication (see arrows). Additionally, some nurse nuclei were unable to correct defects, and dropped out (see triangles).

### Knockdown of *Psf2* displays an S phase delay

Since the truncated *Psf2* displays an M phase delay, we wanted to confirm that the p-element insertion caused a null mutation. Existence of a fully sequenced *Drosophila* genome is pivotal in many modern research techniques. This luxury has allowed for the creation of an RNAi system that knocks out individual proteins in a tissue specific manner. Utilizing the GAL4-UAS system, the GAL4 activation domain is inserted behind a tissue specific enhancer region (31). Activation of the GAL4 domain with the presence of the UAS elements triggers recruitment of RNA polymerase, and the transcription of the RNAi construct (31). This leads to knockdown of proteins within the specific tissue. Use of this technique allows for in vivo analysis of fully depleted proteins that would normally be impossible due to lethality (31). Therefore, we knocked down levels of *Psf2* in normal cycling larval brains using RNAi to observe the phenotype. First, brains were dissected out of 3<sup>rd</sup> instar wandering larvae with depleted levels of *Psf2*, squashed and stained with DAPI for observation. Surprisingly, RNAi knockdown of *Psf2* displays an S phase delay quantified using mitotic indices (Figure 16a). Wildtype larval brains had an average mitotic index of 0.38% while RNAi knockdown lead to an average mitotic index of 0.04%. T-test analysis revealed a statistically significant difference with a p-value of 0.02. In order to confirm the S

phase delay of the cell cycle, the 3<sup>rd</sup> instar larval brains were treated with EdU for incorporation into cells undergoing S phase of the cell cycle. Whole brains were then stained with a fluorescently tagged azide and Hoescht for visualization. After imaging, the RNAi flies displayed more cells incorporating EdU compared to wildtype, confirming the S phase delay when levels of Psf2 are knocked down (Figure 16b).

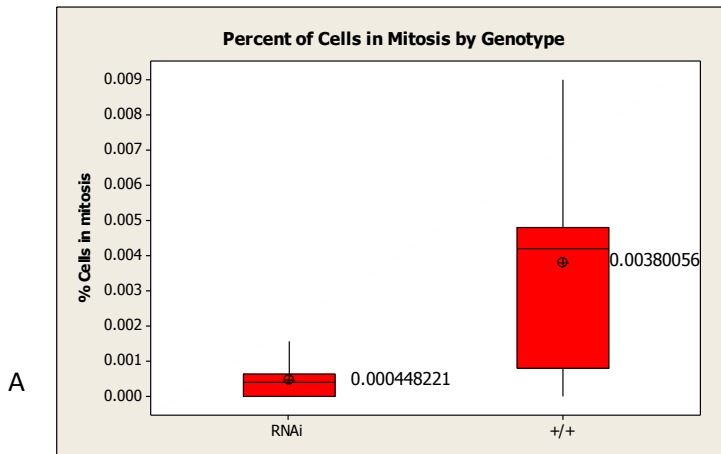
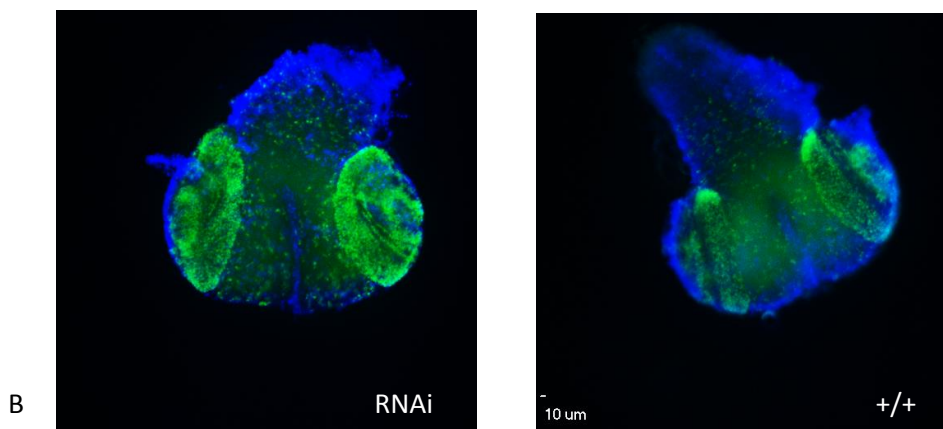


**Figure 16. RNAi Knockdown of Psf2 Leads to an S Phase Delay.** a) 3<sup>rd</sup> instar larval brains were squashed and stained with DAPI. Mitotic figures for wt and RNAi knockdown flies were counted and divided by the number of cells in interphase. RNAi knockdown of Psf2 displays decreased numbers of mitotic figures compared to wildtype. B) Using EdU incorporation to observe the number of cells in S phase in 3<sup>rd</sup> instar wandering larval brains reveals an increased number of cells in S phase in the RNAi knockdown flies compared to wildtype (green).



### Psf2 interacts with Sld5 and Mcm2 confirmed using Yeast Two-Hybrid Analysis

The GINS complex is a ring shaped structure composed of 4 subunits: Psf1, Psf2, Psf3, and Sld5. Previous data confirmed the order of subunits in the ring as Sld5, Psf1, Psf3 and Psf2: showing an interaction between Sld5 and Psf2, and Psf2 and Psf3 (17). In order to confirm the interaction with Sld5, cDNA from *psf2* and *sld5* were cloned into the pGADT7 and pGBKT7 vectors in order to fuse Psf2 and

Sld5 respectively to either the Gal4 activating domain or the Gal4 binding domain. Psf2 and Sld5 in their respective vectors were transformed into the AH109 mutant yeast strain, and plated on media supplemented with histidine as a control, and on media lacking histidine to indicate an interaction. A physical interaction between Psf2 and Sld5 would lead to the recruitment of the RNA polymerase allowing transcription to occur on media lacking histidine. Yeast was grown at 30°C for 2 days, where growth of the yeast strain occurred on the plate lacking His, confirming the previous data of the Psf2-Sld5 interaction (Figure 17).

Mcm2-7 is a 6 subunit complex originally identified in *S. cerevisiae* that binds DNA in early G1 phase. After phosphorylation, the helicase activity of the Mcm2-7 complex is activated (10). Additionally, the GINS complex, in conjunction with Cdc45, has been implicated in increasing the helicase activity of the Mcm2-7 complex (1). Since the GINS complex is assumed to interact with Mcm2-7, we wanted to test the interaction between Psf2 and other subunits of the MCM complex. Using the same method previously discussed, we found a novel interaction between Psf2 and Mcm2 (Figure 17).

In addition to testing for physical interaction between the different proteins, we also used a semi-quantitative approach to test for the strength of interaction between each protein. Using a 5 fold dilution of a 2 day overnight yeast culture, the yeast was grown out to 6 dilutions. The interaction between Mcm2 and Psf2 was strong, visible in the growth all the way to the 6<sup>th</sup> serial dilution, while the interaction between Sld5 and Psf2 was slightly weaker only growing the 4<sup>th</sup> serial dilution (Figure 17).

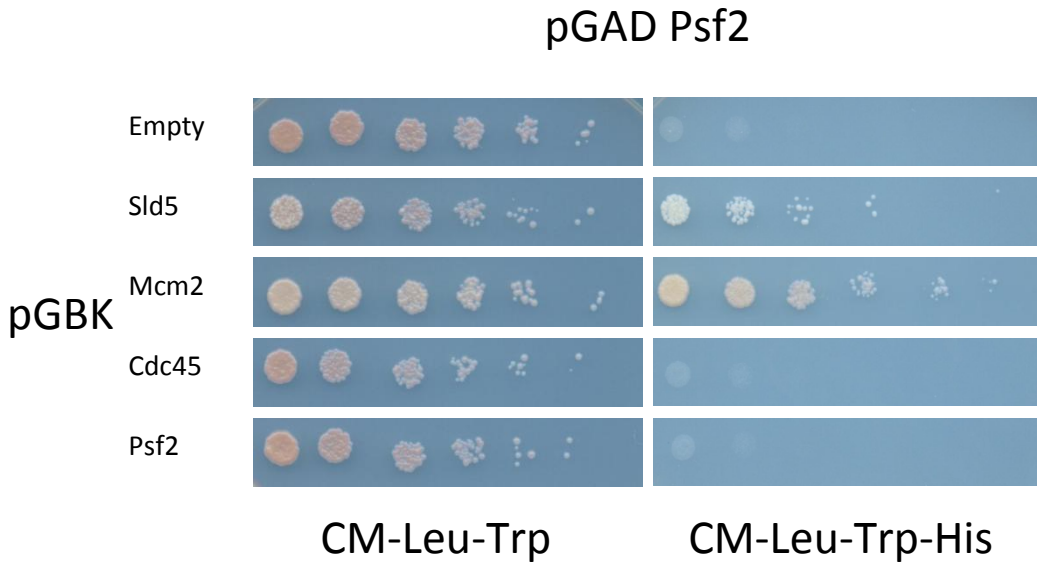


**Figure 17. Yeast Two-Hybrid Analysis of Psf2 Interactions.** Yeast two-hybrid assay for interaction displays interactions with Psf2 and Sld5, Mcm2. Control plated on media supplemented with Histidine (left column) shows growth for each of the vectors. Experimental plated on media lacking Histidine shows growth only with interacting proteins. Psf2 tested with empty pGBK vector as a negative control. Serial dilutions give insight into the strength of the interaction with Mcm2 growing out to the 6<sup>th</sup> serial dilution with Sld5 displaying a slightly weaker interaction with Psf2.

## V. Discussion

Identification of a Psf2 mutant fly line with a C-terminal truncation has helped to provide insight into the complications of removal of that last alpha helical region responsible for Psf2-Psf3 interaction (18). Since the Psf2 homozygous mutant contains two copies of the mutated allele, it is hypothesized that the GINS complex is incapable of forming, preventing the completion of DNA replication, and the inability of the cell to survive. Our data supports this hypothesis since homozygous Psf2 mutants arrest during late embryonic development after the levels of Psf2 from maternal loading are exhausted. Curiously, these cells seem to be arresting in M phase of the cell cycle, contrary to the fact that the removal of GINS leads to a stalled replication fork, and the downregulation of GINS leads to an S phase delay (32). However, previous research on other replication proteins, such as Cdc6, has shown that the

cell cycle will still progress through S phase without the complete replication of the genome, causing an M phase arrest (33).

Analysis of homozygous Psf2 mutant early embryos displays asynchronous nuclei at the periphery, indicating a defect in either M phase or S phase of the cell cycle. Since Psf2 is a replication protein, removal of the interaction domain between Psf2 and Psf3 could lead to malformation of the GINS complex and a defect in S phase of the cell cycle: visible through these asynchronous nuclei. Additionally, the presence of anaphase bridges in the early embryos reinforces the idea that the cell cycle is progressing before the completion of DNA replication, and moving into an unsuccessful M phase.

Since Psf2 is involved in DNA replication throughout S phase of the cell cycle, removal of Psf2 should lead to a significant S phase delay (32). However, observation of regular cycling larval brain in heterozygous mutants reveals an M phase delay. Additionally, defects in mitotic figures such as aneuploidy and broken chromosomes all point to problems during mitosis. Some replication proteins such as ORC and Cdc6 have been shown to display defects in chromosome dynamics during mitosis due to the incomplete replication of the chromosomes (33). Another possible scenario deals with the regulation of the progression of DNA replication during S phase. After the orientation of the replication machinery, multiple proteins such as Chk1, Rad53 (yeast analogue of Chk2), and Mec1 are active during S phase with multiple functions. One of these functions is to retard the progression of the replication fork. This allows for the replication forks that are activated later in S phase to complete replication before exiting S phase (34). Since many of the abnormal phenotypes present in the Psf2 mutant are defects in M phase, contrary to fact that Psf2 is a replication protein present in S phase, it is possible that Psf2 interacts with one of these checkpoint proteins during replication. Therefore, the inhibition of this interaction in the mutant could prevent the retardation of S phase, and the entry into mitosis before

complete replication. Additionally, heterochromatin is replicated late in S phase and typically resides around centromeres, which are key mitotic components, so early entry into mitosis could lead to decreased replication of these centromeres, causing the incomplete separation of sister chromatids resulting in aneuploidy and broken chromosome arms. All of which are defects in S phase of the cell cycle that manifest as phenotypic abnormalities during M phase.

Since the heterozygous mutant appears to display defects in S phase that appear as phenotypic abnormalities during M phase, observation of tissues that undergo multiple S phases without mitosis could prove useful in diagnosing the role of Psf2 during replication. Absence of any replication machinery would prove restrictive in the amount of replication in these tissues visible in the size of the nuclei. Observation of endoreplicating tissue in the heterozygous mutants confirms this hypothesis that Psf2, as a replication protein, is essential for endoreplicating tissue to adequately increase their genomic content. The decreased size of the polytene chromosomes in the salivary tissue of the larvae, as well as the decreased size and abnormal shape of the nurse cells in the heterozygous Psf2 mutant point to a pivotal role for Psf2 and GINS in endoreplicating tissue. Also, the inability of the nurse cell chromosomes to decondense after the characteristic 5-blob stage hints at a role for Psf2 and GINS in chromosome decondensation (30). Again, all phenotypic abnormalities of the Psf2 mutant point to possible defects during S phase of the cell cycle, which would be expected from a replication protein.

Since the Psf2 mutant is homozygous lethal, most of the phenotypic analysis has been performed in heterozygous mutants. Using of the Gal4 driven RNAi knockdown of Psf2 in larval brains, complete knockdown of Psf2 leads to an S phase delay. Since it is hypothesized that the phenotypic abnormalities observed in the heterozygous mutant are a result of the entry into mitosis before complete replication of the genome, indicating Psf2 to be a poision subunit, complete knockdown of Psf2 was expected to demonstrate the same results. Since these results are opposite of what was seen

in the heterozygous mutant, this presents a few possibilities for the role of Psf2 throughout the cell cycle, specifically referring to the function of the C-terminal (Figure 18).

First, the C-terminal truncation does not remove the entire interaction domain between Psf2 and Psf3, so the interaction may simply be weakened. This weak interaction between Psf2 and Psf3 decreases the efficiency of the GINS complex, and replication persists at a slower rate (Figure 18a). Secondly, the C-terminal truncation completely removes the interaction domain between Psf2 and Psf3, but the phenotypes observed are only in heterozygous animals. The inability of Psf2 and Psf3 to interact is imperative to the proper formation of GINS, so the differing results between an M phase and an S phase delay is a dosage effect (Figure 18b). Thirdly, the Psf2-Psf3 interaction domain is completely removed, but the interaction between Psf2 and Psf3 is not required for proper GINS formation. However, this is unlikely since many previous researchers have identified an interaction domain between Psf2 and Psf3, and removal of any of the subunits of GINS results in nonfunctional complex. On the contrary, other previous research has identified fewer interaction domains between Psf2 and other subunits, and propose a horseshoe shaped structure as opposed to the ring shaped (36). Finally, the entirety of the interaction domain has not been removed, Psf2 and Psf3 still interact, and the GINS complex is formed (Figure 18c). Both of these scenarios implicate the C-terminal domain of Psf2 to have functional relevance elsewhere in the cell cycle.

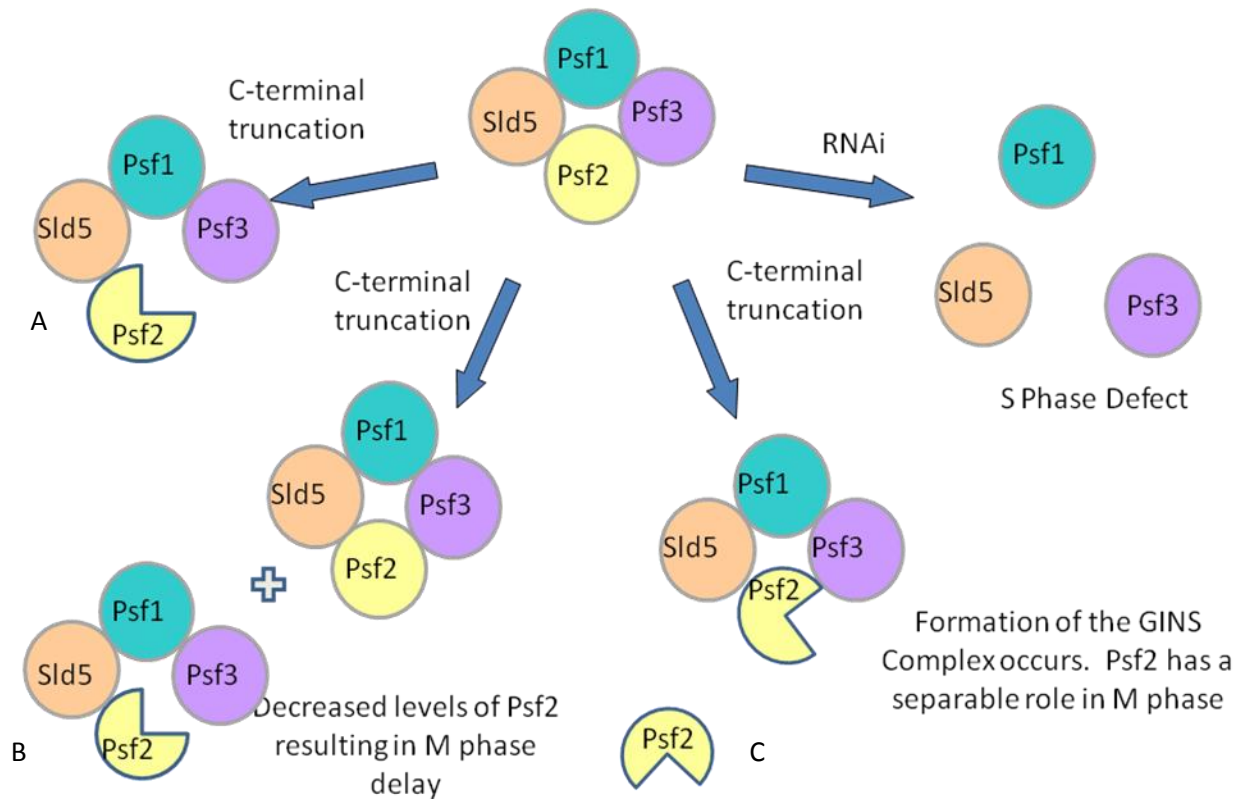


**Figure 18. Schematic Model of Possible Psf2 Mutant Scenarios** a) The interaction between Psf2 and Psf3 is weakened due to the C-terminal truncation, leading to decreased efficiency of GINS. b) The C-terminal truncation inhibits the formation of GINS, but most of the phenotypic abnormalities have been observed in heterozygous mutants. Therefore the differing results are due to a dosage defect. c) The C-terminal truncation does not affect the formation of GINS, implicating a role for the C-terminal of Psf2 elsewhere in the cell.

Previous research in yeast and human tissue cultures has implicated Psf2 to interact with chromosome segregation proteins such as INCENP, Aurora B, and Survivin (4). This research into the role of Psf2 in human chromosome segregation demonstrated the necessity for Psf2 throughout mitosis. siRNA knockdown of Psf2 in human tissue culture cells observed throughout M phase resulted in a 2 hour M phase delay compared to wildtype, and missegregation of proteins aligned at the metaphase plate (4). Additionally, Psf2 was hypothesized to play a role in the attachment of kinetochores to spindle fibers: a function relating to the role of Survivin during mitosis (4). If one of these interaction domains

lies in the C-terminal region truncated in the Psf2 mutant, this could result in the inability of the chromosomes to properly segregate during mitosis. This could account for the aneuploidy and chromosome arm breaks seen in larval brain tissue. Many other replication proteins such as Orc6, Orc2 and Hsk1 have been shown to play dual roles in replication through origin localization and firing, as well as maintaining centromere cohesion of sister chromatids to allow for accurate segregation (37, 38). Therefore, it is likely that Psf2 by itself, or GINS as a functioning complex, also plays a role in mitosis through kinetochore maintenance.

Additionally, in humans, Psf2 has been shown to interact with Chk2. Chk2 plays multiple roles throughout the cell cycle as a checkpoint protein (39, 40). Chk2 is activated during DNA damage to prevent the entry into both M phase and S phase of the cell cycle before DNA damage repair (39, 40). Multiple proteins have been recently identified that are involved in the repair of DNA damage. Any damage occurring prior to the initiation of replication prevents the passage into S phase of the cell cycle (38). However, damage to DNA during S phase results in the stalling of replication forks for repair, and inhibited entry into mitosis (38). If the interaction between Psf2 and Chk2 triggers the stalling of replication forks during DNA damage, inhibition of the interaction between these two proteins would fail to retard or stall the replication fork, and the cell would progress into mitosis. This would lead to multiple complications later in the cell cycle such as an M phase delay or cell death. The resulting defects in M phase of the cell cycle visible in the heterozygous C-terminal mutant could result from inhibited interaction between Psf2 and Chk2.

The accurate formation of the GINS complex is essential for the completion of DNA replication, and progression through the cell cycle (1). Psf2, as a member of the GINS complex, is imperative for this formation, and essential in maintaining genomic stability (16). Additionally, as seen in the truncation mutant, the C-terminal domain of Psf2 is vital for viability, either as a crucial domain for interactions

between each subunit within the GINS complex, or through essential interactions elsewhere in the cell cycle.

## VI. Conclusion

Previous research into the role of Psf2 during S phase and throughout the cell cycle has been briefly studied in many human tissue cultures and yeast. However, this is the first *in vivo* approach to characterize the result of a C-terminal truncation of the Psf2 protein. Through multiple analyses, Psf2 has been shown to play a role in M phase, either through a defect in the formation of the GINS complex and accurate completion of replication, or through a separable role in chromosome segregation and DNA damage checkpoint controls. Additionally, yeast two hybrid analysis has confirmed the previous interaction observed between Psf2 and Sld5, while introducing a novel interaction between Psf2 and Mcm2, a member of the Mcm2-7 helicase.

Further research into the role of Psf2 through its interactions with other proteins such as Chk2, Survivin and Mcm2 would provide useful information in diagnosing the role of Psf2 throughout the cell cycle. Moreover, the specific role of Psf2 is crucial in understanding the functioning of the GINS complex, and its purpose throughout S phase. DNA replication is an intricate process that is still poorly understood. Likewise, defects in the process of replication initiation, elongation and termination create the root of many disease states such as cancer (21). Further insight into the role of the replication machinery could prove useful in the diagnoses and treatment of many diseases.

## VII. References

1. GINS, a novel multiprotein complex required for chromosomal DNA replication in budding yeast.(2003). *Genes & Development*, 17(9), 1153-1165.
2. Tye, B. K. (2000). Insights into DNA replication from the third domain of life. *Proceedings of the National Academy of Sciences of the United States of America*, 97(6), 2399.
3. DNA polymerase alpha, a component of the replication initiation complex, is essential for the checkpoint coupling S phase to mitosis in fission yeast.(1995). *Journal of Cell Science*, 108(9), 3109-18.
4. Huang, H. (2005). Suppressors of Bir1p (survivin) identify roles for the chromosomal passenger protein Pic1p (INCENP) and the replication initiation factor Psf2p in chromosome segregation. *Molecular and Cellular Biology*, 25(20), 9000-9015.
5. Assembly of a complex containing Cdc45p, replication protein A, and Mcm2p at replication origins controlled by S-phase cyclin-dependent kinases and Cdc7p-Dbf4p kinase.(2000). *Molecular and Cellular Biology*, 20(9), 3086-96.
6. Sclafani, R. A. Cell cycle regulation of DNA replication. *Annual Review of Genetics*, 41, 237-280.
7. First the CDKs, now the DDKs.(1999). *Trends in Cell Biology*, 9(7), 249-252.
8. Sheu, Y., & Stillman, B. (2010). The Dbf4–Cdc7 kinase promotes S phase by alleviating an inhibitory activity in Mcm4. *Nature*, 463(7277), 113-117.
9. Bauerschmidt, C., Pollok, S., Kremmer, E., Nasheuer, H., & Grosse, F. (2007). Interactions of human Cdc45 with the Mcm2-7 complex, the GINS complex, and DNA polymerases  $\alpha$  and  $\epsilon$  during S phase. *Genes to Cells*, 12(6), 745-758.

10. Yoshiki, Y., Takuro, N., & Hisao, M. (2004). A novel intermediate in initiation complex assembly for fission yeast DNA replication. *Molecular Biology of the Cell*, 15(8), 3740-50.
11. Christensen, T.W., & Tye, B.K. (2003). Drosophila MCM10 interacts with members of the prereplication complex and is required for proper chromosome condensation. *Molecular Biology of the Cell*, 14(6), 2206-15.
12. Chattopadhyay, S. (2007). Human Mcm10 regulates the catalytic subunit of DNA polymerase- $\alpha$  and prevents DNA damage during replication. *Molecular Biology of the Cell*, 18(10), 4085-4095.
13. Kamada, K., Kubota, Y., Arata, T., Shindo, Y., & Hanaoka, F. (2007). Structure of the human GINS complex and its assembly and functional interface in replication initiation. *Nature Structural and Molecular Biology (Formerly Called Nature Structural Biology)*, 14(5), 388-396.
14. Aparicio, T., Ibarra, A., & Méndez, J. (2006). Cdc45-MCM-GINS, a new power player for DNA replication. *Cell Division*, 1(1), 18-0.
15. Grp/DChk1 is required for G2-M checkpoint activation in drosophila S2 cells, whereas Dmnk/DChk2 is dispensable.(2005). *Journal of Cell Science*, 118(9), 1833-42.
16. De Falco, M., Ferrari, E., De Felice, M., Rossi, M., Hübscher, U., & Pisani, F. M. (2007). The human GINS complex binds to and specifically stimulates human DNA polymerase  $\alpha$ -primase. *EMBO Reports*, 8(1), 99-103.
17. Kanemaki, M., Sanchez-Diaz, A., Gambus, A., & Labib, K. (2003). Functional proteomic identification of DNA replication proteins by induced proteolysis in vivo. *Nature*, 423(6941), 720-725.
18. Chang, Y. P. (2007). Crystal structure of the GINS complex and functional insights into its role in DNA replication. *Proceedings of the National Academy of Sciences of the United States of America*, 104(31), 12685-12690.
19. Crystal structure of the human GINS complex.(2007). *Genes & Development*, 21(11), 1316-1321.

20. A key role for the GINS complex at DNA replication forks.(2007). *Trends in Cell Biology*, 17(6), 271-278.
21. Kanemaki, M., & Labib, K. (2006). Distinct roles for Sld3 and GINS during establishment and progression of eukaryotic DNA replication forks. *The EMBO Journal*, 25(8), 1753-1763.
22. Obama, K., Ura, K., Satoh, S., Nakamura, Y., & Furukawa, Y. (2005). Up-regulation of Psf2, a member of the GINS multiprotein complex, in intrahepatic cholangiocarcinoma. *Oncology Reports*, 3, 701-6.
23. ATM and ATR substrate analysis reveals extensive protein networks responsive to DNA damage.(2007). *Science*, 316(5828)
24. Drosophila Chk2 is required for DNA damage-mediated cell cycle arrest and apoptosis.(2001). *FEBS Letters*, 508(3), 394-398.
25. Walter, B. E., Perry, K. J., Fukui, L., Malloch, E. L., Wever, J., & Henry, J. J. (2008). Psf2 plays important roles in normal eye development in *xenopus laevis*. *Molecular Vision*, 14, 906-921.
26. Drosophila melanogaster: The model organism.(2006). *Entomologia Experimentalis Et Applicata*, 121(2), 93-103.
27. CDC6: From DNA replication to cell cycle checkpoints and oncogenesis.(2008). *Carcinogenesis*, 29(2), 237-237.
28. Expression and function of drosophila cyclin a during embryonic cell cycle progression.(1989). *Cell (Science Direct)*, 56(6), 957-957.
29. Zhang, P., & Spradling, A. (1995). The drosophila salivary gland chromocenter contains highly polytenized subdomains of mitotic heterochromatin. *Genetics*, 139, 659-670.
30. Royzman, I. (1998). S phase and differential DNA replication during drosophila oogenesis. *Genes to Cells*, 3(12), 767-776.

31. Duffy, J. B. (2002). GAL4 system in drosophila: A fly geneticist's swiss army knife. *Genesis: The Journal of Genetics and Development*, 34(1-2), 1-15.
32. The human GINS complex associates with Cdc45 and MCM and is essential for DNA replication.(2009). *Nucleic Acids Research*, 37(7), 2087-2095.
33. Lau, E., Zhu, C., Abraham, R. T., & Jiang, W. (2006). The functional role of Cdc6 in S-G2/M in mammalian cells. *EMBO Reports*, 7(4), 425-430.
34. Tercero, J. A., & Diffley, J. F. X. (2001). Regulation of DNA replication fork progression through damaged DNA by the Mec1/Rad53 checkpoint. *Nature*, 412(6846), 553.
35. Lee, H. O. (2009). Endoreplication: Polyploidy with purpose. *Genes & Development*, 23(21), 2461-2477.
36. Boskovic, J., Coloma, J., Aparicio, T., Zhou, M., Robinson, C. V., Méndez, J., et al. (2007). Molecular architecture of the human GINS complex. *EMBO Reports*, 8(7), 678-684.
37. Orc mutants arrest in metaphase with abnormally condensed chromosomes.(2001). *Development*, 128(9), 1697-707.
38. Raveendranathan, M., Chattopadhyay, S., Bolon, Y., Haworth, J., Clarke, D. J., & Bielinsky, A. (2006). Genome-wide replication profiles of S-phase checkpoint mutants reveal fragile sites in yeast. *The EMBO Journal*, 25(15), 3627-3639.
39. Drosophila Chk2 is required for DNA damage-mediated cell cycle arrest and apoptosis.(2001). *FEBS Letters*, 508(3), 394-398.
40. Rad53 regulates replication fork restart after DNA damage in *saccharomyces cerevisiae*.(2008). *Genes & Development*, 22(14), 1906-1920.
41. Apger, Jennifer, Reubens, Michael, Henderson, Laura, Gouge, Catherine A., Ilic, Nina, Zhou, Helen H., and Christensen, Tim W. Multiple Functions for *Drosophila Mcm10* Suggested

Through Analysis of Two *Mcm10* Mutant Alleles. *Genetics* 2010; published ahead of print on May 24, 2010 as doi: [10.1534/genetics.110.117234](https://doi.org/10.1534/genetics.110.117234)

## VIII. Appendix I

### Optimization of Psf2 Antibody using Western Blots

#### Materials and Methods

Embryos were collected from wildtype and *psf2* mutant fly lines on grape agar plates after 12 hours by squirting water on the grape agar (Genesee Scientific™) plate, swirling embryos around with a small paint brush, and removing embryos from plate using a p1000 pipette. Embryos were placed in a 1.5mL Eppendorf tube, water was immediately removed, and the embryos were stored at -80°C. For the Western Blot, embryos were removed from storage and 3X SDS PAGE loading buffer was added to the embryos to equal a concentration of 55.5 mg/μL. Embryos were then ground up using a grinder and placed in boiling water for 10 minutes. After 10 minutes, embryos were removed and placed in a centrifuge at 13.3 for 5 minutes. Protein extracted from Psf2 and wildtype embryos was then added to a 12% protein gel (Pierce™) in varying amounts: 8μL, 12μL, and 16μL. 5 μL of the EZ Run Pre-stained ladder™ (Fisher™) were added to each side of the protein lanes. Gel was run at 72 volts with 1 X HEPES (Pierce™) running buffer (Table 7) until the protein reached the bottom of the gel. While the gel was running, a 6.5 X 8 silicon membrane was covered in methanol until all the white was removed, and immersed in Transfer Buffer (Table 8). After the gel was finished running, 6 pieces of transfer buffer soaked blotter paper was placed on the bottom of the transfer machine followed by the membrane, the gel, and 6 more pieces of transfer soaked blotter paper. Transfer of protein from the gel to the membrane was run at 33mAmps for 3 hours. Once transferred, the membrane was placed in a blocking solution (10% milk in Washing Buffer) for 1 hour. After blocking, membrane was placed in primary antibody solution (1:50 anti-Psf2 Chicken (Pacific Immunology™) in 10% milk solution) and incubated at 4°C overnight. Following primary antibody incubation, membrane was removed and placed in the

Washing Buffer (Table 9) for 3 hours, changing the Buffer every 30 minutes. After washing the primary antibody, the membrane was placed in the secondary antibody solution (1:5000 anti-Chick (Millipore™) conjugated to HRP in 10% milk solution) and incubated at 4°C for 45 minutes. After 45 minutes, secondary antibody solution was washed in Washing Buffer for 2 hours, changing solution every 30 minutes. After washing, Membrane was placed in HRP chemiluminescent solution (Millipore™) for 1 minute. Membrane was then placed between two transparencies and imaged at a 45 minute exposure time.

**Results:** Psf2 antibody revealed the presence of Psf2 in both wildtype and heterozygous Psf2 mutants. However, nonspecific binding and decreased affinity made it difficult to determine if the truncated Psf2 was present in the mutant (Figure 19).

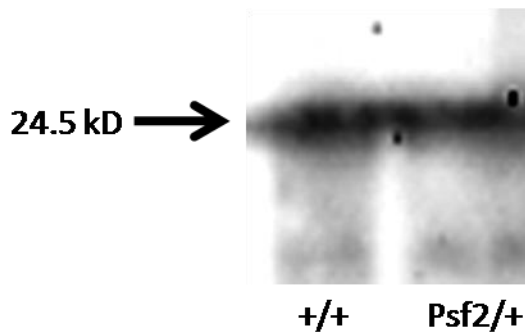


**Figure 19. Western Blot of Psf2** Psf2 antibody detected Psf2 protein present in wildtype and heterozygous mutant.

Component	Amount Added
Tris Base	121 g
HEPES™ (Pierce™)	238 g
SDS	10 g

dH <sub>2</sub> O	to 1000 mL
-------------------	------------

Table 7. Components of 10X HEPES Running Buffer. Diluted to 1X for use

Component	Amount Added
Tris Base	5.8 g
Glycine	2.9 g
10% SDS	3.7 mL
MetOH	200 mL
dH <sub>2</sub> O	to 1000 mL

Table 8. Components of Transfer Buffer

Component	Amount Added
10X PBS	100 mL
Tween-20	2 mL
dH <sub>2</sub> O	to 1000 mL

Table 9. Components of Washing Buffer

## IX. Appendix II

### Mcm10 Mutations cause defects in chromosome condensation visible in *Drosophila* Ovaries

#### Materials and Methods

**Ovary/Follicle Dissection and Imaging:** Female fly stocks of *Mcm10*<sup>scim19</sup> homozygous mutant and *Mcm10*<sup>d08029</sup> homozygous mutant 3-7 days post eclosion were fed for 2 days with a 1:1 mixture of active dry yeast and dH<sub>2</sub>O. Random female flies were selected, and ovaries were dissected out in a dual concavity slide in one well with 50  $\mu$ L 1X PBS. Ovarioles were teased apart using a needlepoint tool, moved to the second well, and fixed for 20 minutes in a 4% Formaldehyde in PBX (PBS with 1% Triton X-100). After fixing, ovaries were moved to a new well and stained for 5 minutes in a 1  $\mu$ g/ml DAPI in PBS. Ovaries were then washed 3X in PBX, followed by a 1 hour PBX wash, and 3X 10 minute washes in PBX. Ovaries were then moved using Dumoxel™ Tweezers #5 (Electron Microscopy Sciences™) to a clean Lifterslip™ (Thermo Scientific™), mounted with Vectashield™ (Vector™) and imaged using confocal optical sectioning microscopy.

**Results:** Jennifer Apger, Michael Reubens, Laura Henderson, Catherine A. Gouge, Nina Ilic, Helen H. Zhou, and Tim W. Christensen. Multiple Functions for *Drosophila* *Mcm10* Suggested Through Analysis of Two *Mcm10* Mutant Alleles. *Genetics* 2010; published ahead of print on May 24, 2010 as doi: 10.1534/genetics.110.117234 (Figure 20).

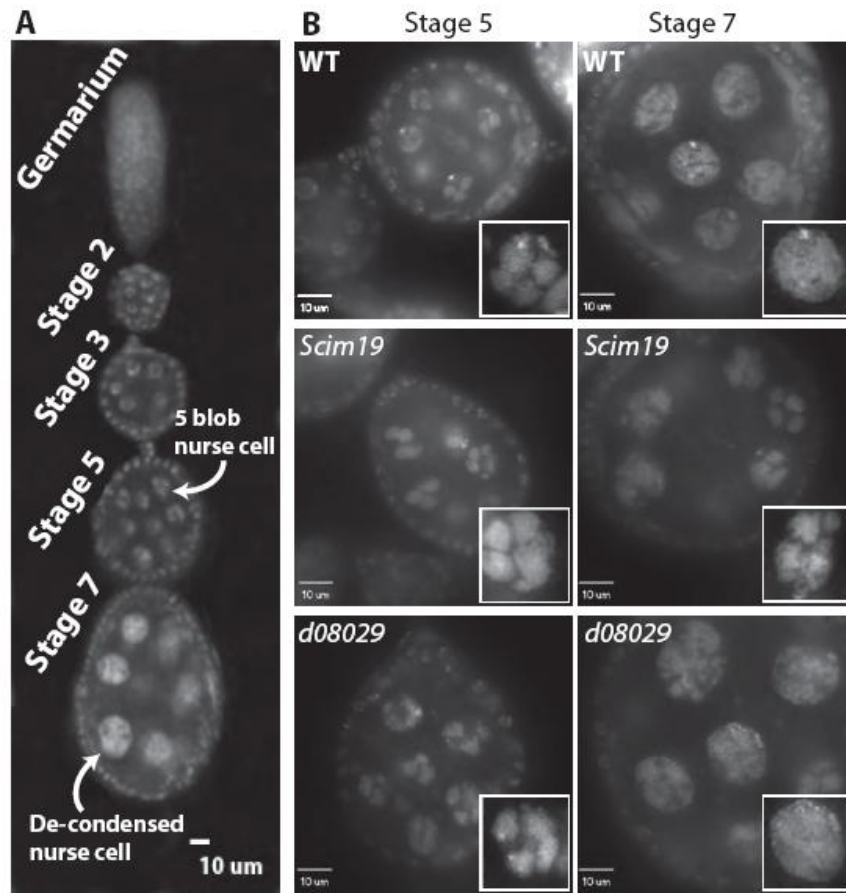


**Figure 20. Condensation Defects Visualized in *Mcm10* Mutant Ovarioles.** Analysis of ovaries in *Mcm10scim19* homozygous mutant revealed an inability to decondense from the 5 blob stage compared to wildtype. However, the homozygous truncation mutant, *Mcm10d08029*, progressed through the stages of development with no defects. ( Jennifer Apger, Michael Reubens, Laura Henderson, Catherine A. Gouge, Nina Ilic, Helen H. Zhou, and Tim W. Christensen. Multiple Functions for *Drosophila Mcm10* Suggested Through Analysis of Two *Mcm10* Mutant Alleles. *Genetics* 2010; published ahead of print on May 24, 2010 as doi: 10.1534/genetics.110.117234 )

## X. Appendix III

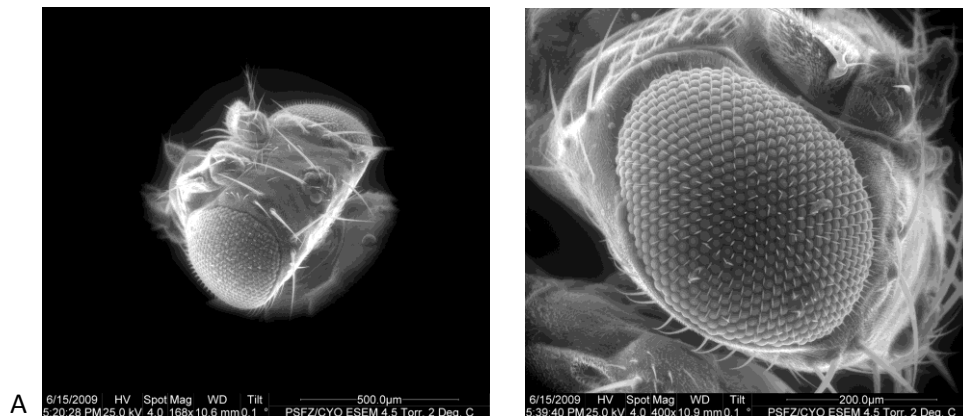
### RNAi knockdown of Psf2 leads to defects in formation of *Drosophila* eyes

#### Materials and Methods

RNAi knockdown of Psf2 in eye tissue of flies was initiated by crossing Psf2 RNAi line virgins with the GAL4 driver for RNAi knockdown in eye tissue. F1 progeny were observed under a dissecting light microscope for phenotypic abnormalities. Flies exhibiting defects in eye formation were frozen and observed through scanning electron microscopy. Psf2/CyO mutant fly lines were also observed under a dissecting light microscope, and random female and male flies were chosen for observation through scanning electron microscopy for comparison.

#### Results

Psf2/CyO mutants displayed no visible defects in eye development (Figure 21a). RNAi knockdown of Psf2 in eye tissue displays defects in eye development. A mutated area appears on the ventral side of the left eye, forcing the eye to be located more towards the dorsal side of the head (Figure 21b). Additionally, there is an extra antennae located on the anterior of the head (Figure 21c), as well as mutated bristles (Figure 21d).



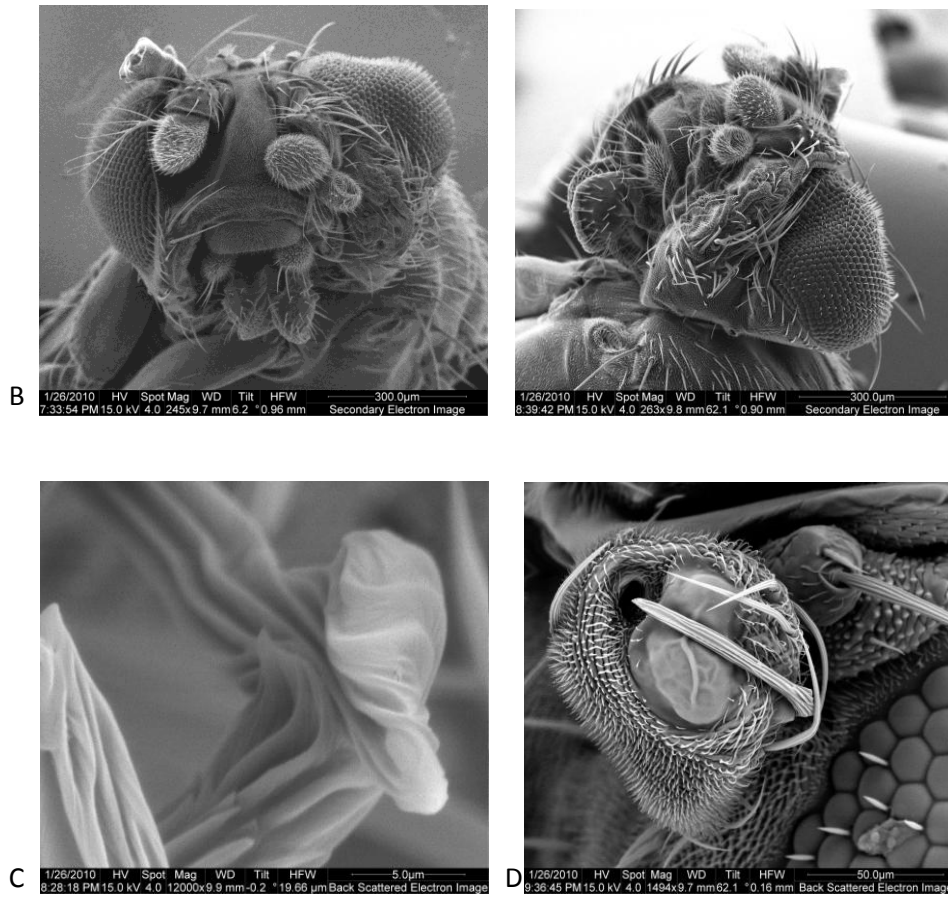


**Figure 21. Mutated Eye Region Resulting from Psf2 RNAi Knockdown.** a)

Psf/CyO flies display no defects in eye development. b) RNAi knockdown of Psf2 in eye tissue displays a mutated area located on the ventral side of the head. The eye has been moved dorsally. c) Bristles located on the RNAi fly are bent, with irregular grooves. d) An extra antenna appears on the anterior of the head in the RNAi flies.

## XI. Appendix IV

### Generation of Psf2 null mutant flies using imprecise p-element excision

Null mutant flies were generated using the cross seen in Figure 22. Final stocks were observed to see if you curly was lost.

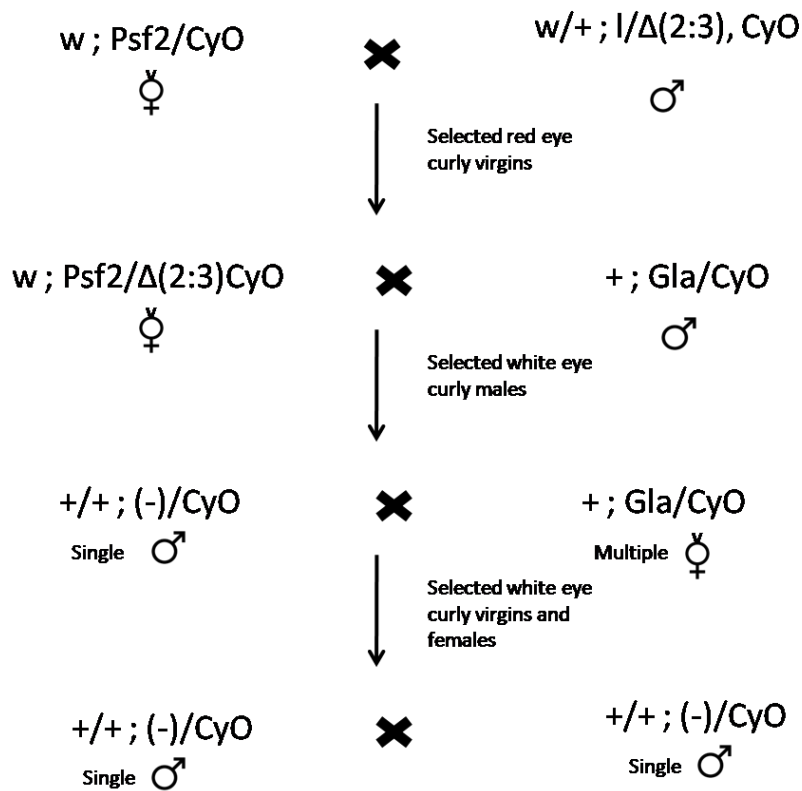


Figure 22. Generation of a Psf2 null mutant using imprecise p-element excision

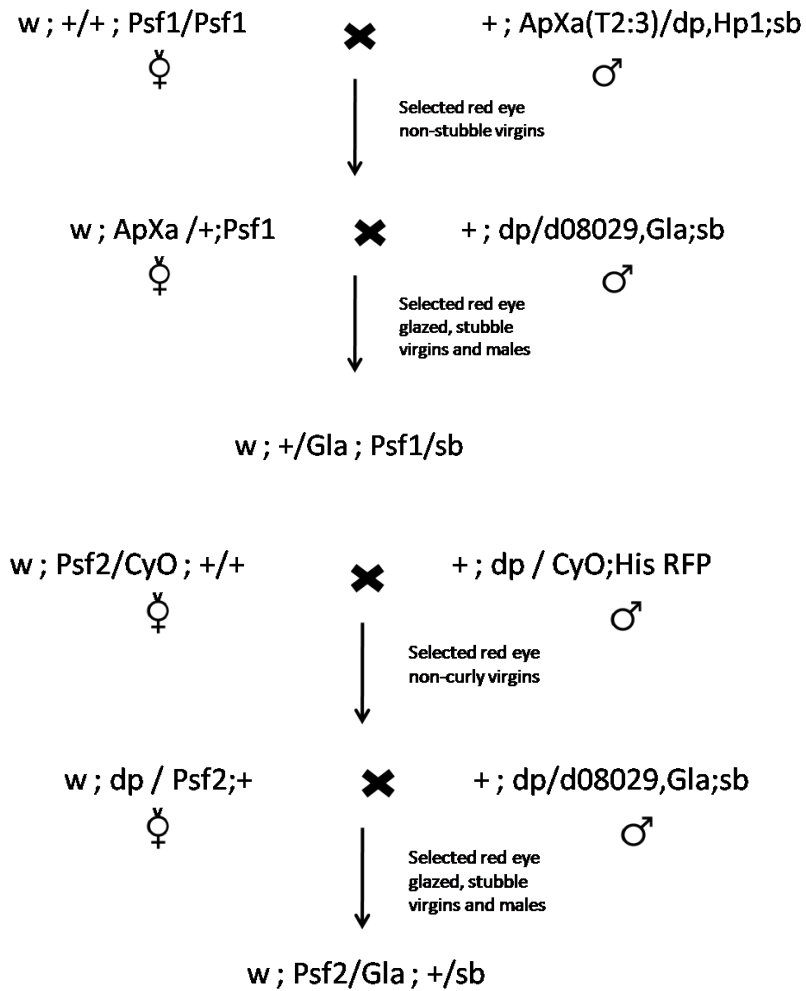
**Results:** 7 lines were unable to lose the curly balancer, but further analysis is necessary to determine if there is a Psf2 null mutation.

## XII. Appendix V

### Generation of double mutant flies

#### Materials and Methods

The Psf2-Psf1 double mutant fly was generated as seen in Figure 23.



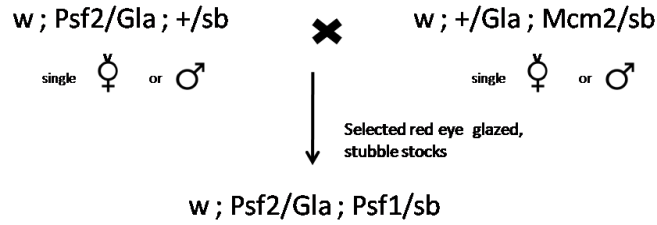
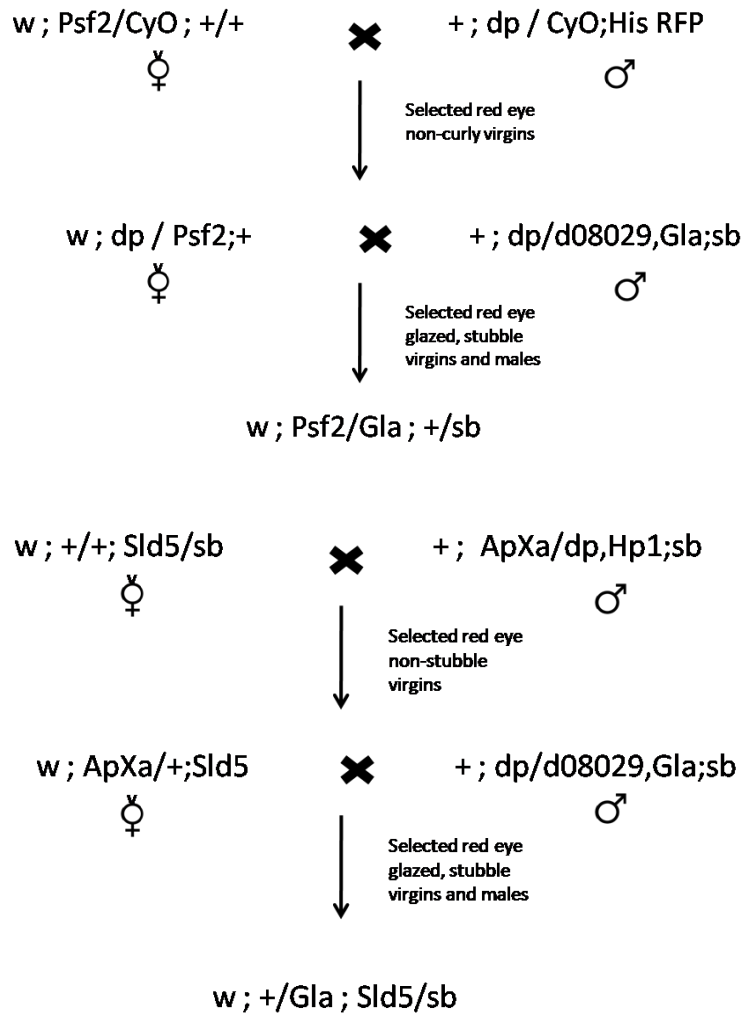


Figure 23. Generation of Psf2-Psf1 double mutant fly

The Psf2-Sld5 double mutant fly was generated as seen in Figure 24.



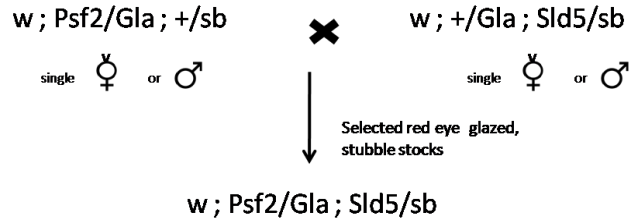
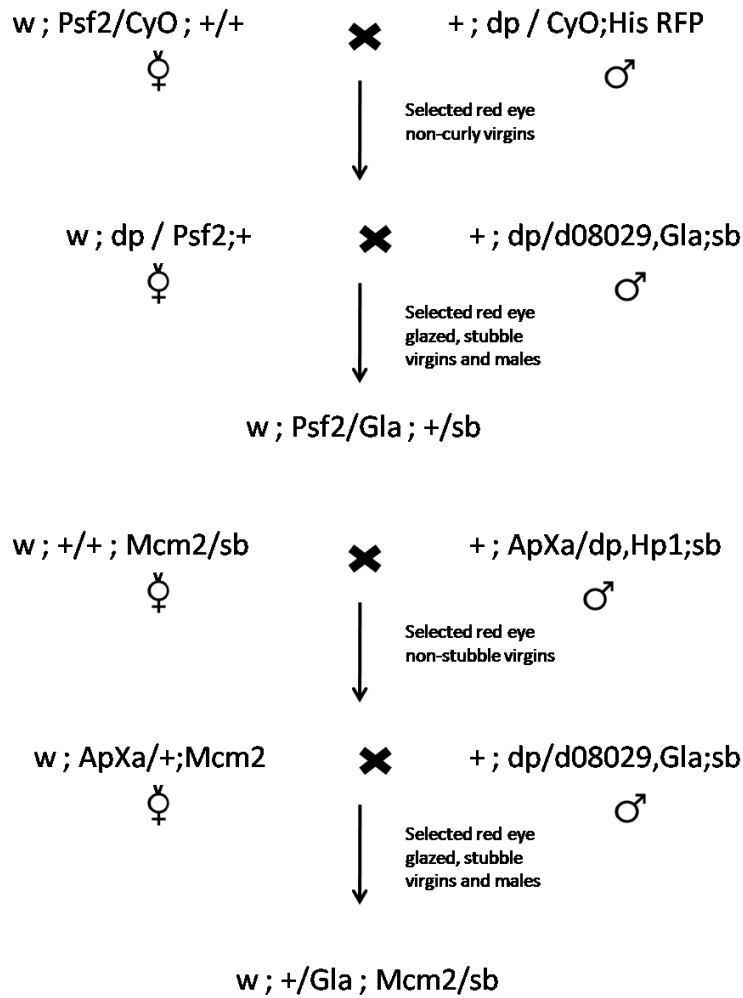


Figure 24. Generation of Psf2-Sld5 double mutant fly

The Psf2-Mcm2 double mutant was generated as seen in Figure 25.



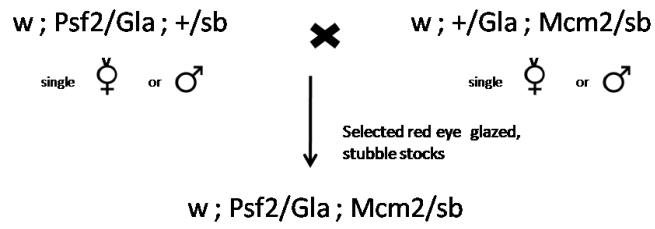


Figure 25. Generation of Psf2-Mcm2 double mutant fly

### XIII. Appendix VI

#### PEV Analysis of Psf2 heterozygous mutant

**Methods:** A cross was performed to observe the role of Psf2 in silencing of heterochromatin (Figure 26).

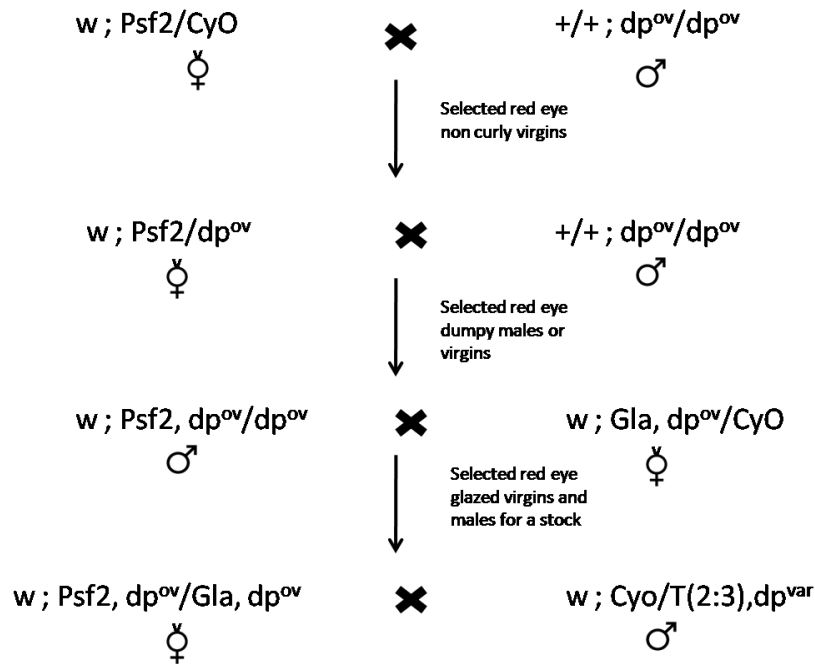
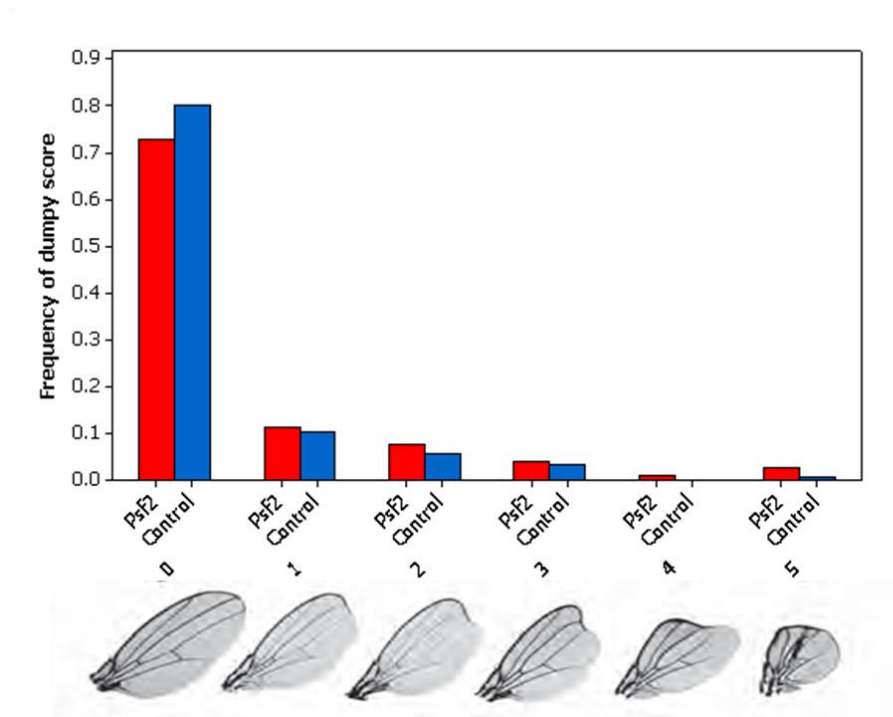


Figure 26. Psf2 position effect variegation cross

Following the cross to the variegating line, flies were scored according to the severity of the dumpy phenotype, with a built-in control.

**Results:** The analysis allowed for the determination of the distance from the centromere where heterochromatin formation occurred. The mean dumpy score for the control was 0.344 and the mean dumpy score for Psf2 was 0.57 (Figure 27b). T-test analysis using Minitab™ statistical software showed a significant increase in variegation in the Psf2 mutant line with a p-value of .008.

**Discussion:** Heterochromatin is replicated late during S phase and contains silenced regions of the genomes (41). Alterations in the formation of heterochromatin can result in changes of genomic expression. Since the *psf2* heterozygous mutant reveals an increase in variegation, there is more heterochromatin formation occurring in the mutant compared to the control. This could result from the retardation of replication elongation due to decreased levels of the GINS Complex, resulting in an increase in late replication of DNA, which leads to increased formation of heterochromatin.



**Figure 27. Position Effects Variegation Analysis of Psf2.** Flies were scored to reveal and increase in the number of flies expressing the dumpy gene, indicating a decrease in the formation of heterochromatin. Statistical analysis revealed an increase in variegation in the heterozygous mutant which was statistically significant with a p-value of 0.008

